VOLUMETRIC CHANGE OF SILTS FOLLOWING CYCLIC LOADING

Christopher D. P. Baxter, Ph.D., P.E.
Jan Trautman
Oliver-Denzil S. Taylor, Ph.D., P.E.

University of Rhode Island
June 2013

URITC PROJECT NO. 500230600000001851

FINAL REPORT

PREPARED FOR

UNIVERSITY OF RHODE ISLAND
TRANSPORTATION CENTER

1. Report No	2. Government Accession No.	3. Recipient's Catalog No.
URITC FY08-09		

4. Title and Subtitle	5. Report Date
Volume Change of Silts Following Cyclic Loading	June 21, 2013
	6. Performing Organization Code: N/A

7. Authors(s)	8. Performing Organization Report No.
Christopher D.P. Baxter, Jan Trautmann, and Oliver-Denzil S. Taylor	N/A

9. Performing Organization Name and Address	10. Work Unit No. (TRAIS)
Departments of Ocean/Civil and Environmental Engineering University of Rhode Island Narragansett, RI 02882-1197	N/A
	11. Contract or Grant No.: URI 0001851
	13. Type of Report and Period Covered: Final

12. Sponsoring Agency Name and Address	14. Sponsoring Agency Code
University of Rhode Island Transportation Center Carlotti Administration Building, 75 Lower College Rd Kingston, RI 02881	

15. Supplementary Notes
N/A

16. Abstract

Estimating the settlement of adjacent structures during pile installation in silts is a challenging problem for practicing engineers. The current state-of-practice relies primarily on local case studies and monitoring efforts, such as inclinometers and site surveys, where adjacent structures are in relatively close proximity to pile driving activity. Few predictive models exist to aid engineers, and those that do exist are limited to relatively "clean" sands and are rarely used in practice. A very important aspect of pile driving are the shear waves that will be generated causing localized regions of increased pore pressures resulting in significant reduction of soil strength and stiffness. Unfortunately, current practice does not provide an engineer with any quantifiable means to estimate how these shear waves would affect the local soil behavior.

The objective of this study was to perform a detailed review of the literature regarding pile driving-induced settlements and to develop a laboratory testing program to quantify the relationship between cyclic loading, generation of pore pressures, and the resulting volume changes in silts.In the first part of the present work a review of case studies and a summary of settlement prediction methods are presented and the most important facts concerning those are highlighted. The second part focuses on a series of cyclic triaxial tests carried out to evaluate volumetric change caused by pore pressure dissipation of silt samples following cyclic loading. It was found that the greater the pore pressure ratio generated during cyclic loading, the greater the volume changes of the silt sample resulting from pore pressure dissipation. Cyclic loading and drainage caused a maximum of 5% volumetric strain in the silt samples, compared to less than 1% for sands in comparable studies. The measured increase in volumetric strain was small up to a pore pressure ratio of 0.6. The results of this research work supply important information on the behavior of volume changes of silt cyclically loaded and provide a sound basis for future settlement predictions of silt due to dynamic loading.

17. Key Words	18. Distribution Statement
Silts, cyclic loading, volume change, pile driving	No restrictions. This document is available to the Public through the URI Transportation Center, Carlotti Administration Building, 75 Lower College, Rd., Kingston, RI 02881

19. Security Classif. (of this report)	20. Security Classif. (of this page)	21. No. of Pages	22. Price
Unclassified	Unclassified	44	

Table of Contents

List of Figures

List of Tables

1. Introduction

This study is part of a larger project funded by the Rhode Island Department of Transportation and the URI Transportation Center to develop a methodology for predicting the settlement of adjacent ground that can occur from pile driving in silts. The proposed approach for conducting this study was originally divided into three distinct phases: (1) a detailed review of various case studies where deformation was observed; (2) a laboratory testing of the dynamic behavior of silts; and (3) the development and validation of a constitutive model to estimated settlements. This report documents work accomplished on the first two objectives. Specifically this report provides a detailed review of literature regarding pile driving-induced settlements and the development a laboratory-testing program to quantify the relationship between cyclic loading, generation of pore pressures, and the resulting volume changes in silts. The development and validation of a constitutive model to estimate settlement will be the focus of a different report.

Estimating the settlement of adjacent structures during pile installation in silts is a challenging problem for practicing engineers. The current state-of-practice relies primarily on local case studies and monitoring efforts, such as inclinometers and site surveys, where adjacent structures are in relatively close proximity to pile driving activity. Few predictive models exist to aid engineers, and those that do exist are limited to relatively "clean" sands and are rarely used in practice.

A very important aspect of pile driving is the shear waves that are generated causing localized regions of increased pore pressures resulting in significant reduction of soil strength and stiffness. This reduction in soil properties can potentially lead to significant settlements and liquefaction. Additionally, after driving, the dissipation of the generated pore pressures results in soil densification and additional settlements. This is of particular significance for urban areas in Rhode Island, which are underlain by thick layers of non-plastic silts prone to liquefaction. It is known that there have been several cases of large settlements in adjacent soils occurring in Providence following the installation of piles or sheet piles. Unfortunately, current practice does not provide an engineer with any quantifiable means to estimate how these shear waves would affect the local soil behavior. Nor does the method estimate the extents of influence of the localized shear waves.

The objectives of this study were to (1) perform a detailed review of various case studies where settlement (deformation) was observed and (2) carry out an experimental program of the dynamic behavior of silts. An approach similar to that of Lee and Albasia (1974) and Ishihara and Yoshimine (1992) was employed, in which samples were loaded to a specific number of cycles or pore pressure ratio, and then allowed to consolidate under constant effective stress. The pore pressure ratio was then related to the volume change of the samples. This data will be used, later on, for developing the constitutive model to predict settlement.

2. Literature Review

This chapter presents a literature review of settlement caused by pile driving, with a particular emphasis on silty soils where possible. Case studies are first summarized, followed by a review of methods used to predict settlements due to pile driving.

2.1 Case Studies Involving Settlement of Adjacent Ground due to Pile Driving

There are a number of reported cases of settlement caused by pile driving, and this section summarizes studies where significant movement of adjacent structures was observed and documented (Table 1).

Table 1: Overview of case studies

Reference	Location
Dalmatov, Ershov and Kovalevsky (1968)	Leningrad, Russia
Clough and Chameau (1980)	Embarcadero, San Francisco, USA
Picornell and del Monte (1982)	Leska, Spain
Lacy and Gould (1985)	Review of 9 sites in northeastern USAand 10 cases from literature reviews
Linehan, Longiow and Dowding (1992)	Northbrook pipeline, Illinois, USA
Leathers (1994)	Back Bay, Boston, USA
Bradshaw, Miller and Baxter (2007)	Providence, Rhode Island, USA

(Listed by authors, year published and location)

2.1.1 Dalmatov, Ershov and Kovalevsky (1968)

The authors described two cases of settlement caused by pile driving in Leningrad, Russia in 1966: one from sheet pile driving and the other from pile driving.In the first case, 70 steel sheet piles were driven 8m deep into the soil adjacent to other buildings. The sheeting was installed at a distance of 1.65 m from a continuous footing and of 1.0 m from two column footings. It was found that no building settlements occurred when the distance between the sheet piles and the continuous footing exceeded 7m. For the second case, settlement of a water main was measured. The water main was a cast-iron, 750mm diameter pipe located at a depth of 3.25m below ground. Hollow,reinforced concretepipe piles (600mm diameter) were driven to a depth of 24m at a distance of 22 to 25m from the water main. The piles were driven using an impact hammer with an energy transfer of 34,000 N-m. The soil at this site was random fill (building waste and organic and natural glacial soil) and no settlement of the water main was observed even though accelerations as large as 200 mm/sec^2 were measured.

The authors were of the opinion that, once accelerations reached a critical value, the soil would compact and settlement of the foundation would occur. They stated that this critical acceleration was governed by the ability of the soil to withstand the influence of vibration without volume change. If the critical acceleration and the attenuation of the acceleration for a

site were known, it would be possible to determine the boundaries of a zone, outside which no settlement would occur. Maslov (1959) and Ershov (1965) estimated the numerical values of critical acceleration by results of laboratory experiments for the two cases of settlement. They concluded that if the observed accelerations where smaller than the critical accelerations there were no dynamic foundation settlements.

2.1.2 Clough and Chameau (1980)

Settlement due to sheet pile driving in San Francisco, California is described in this case study. In 1977, a new storm water storage and transport culvert system was installed in the Embarcadero area. Part of the construction was the installation of braced sheet pile walls, which were installed using a vibratory hammer. The ground conditions consisted of 9m of fill (dune sand, rock fragments, bay mud, general refuse and debris and ship bulk) overlying, soft bay mud and alternating layers of dense sand and firm clay. The water table was 1.5-3.0m below ground surface. An idealized soil profile of the Embarcadero area is shown in Figure 1.

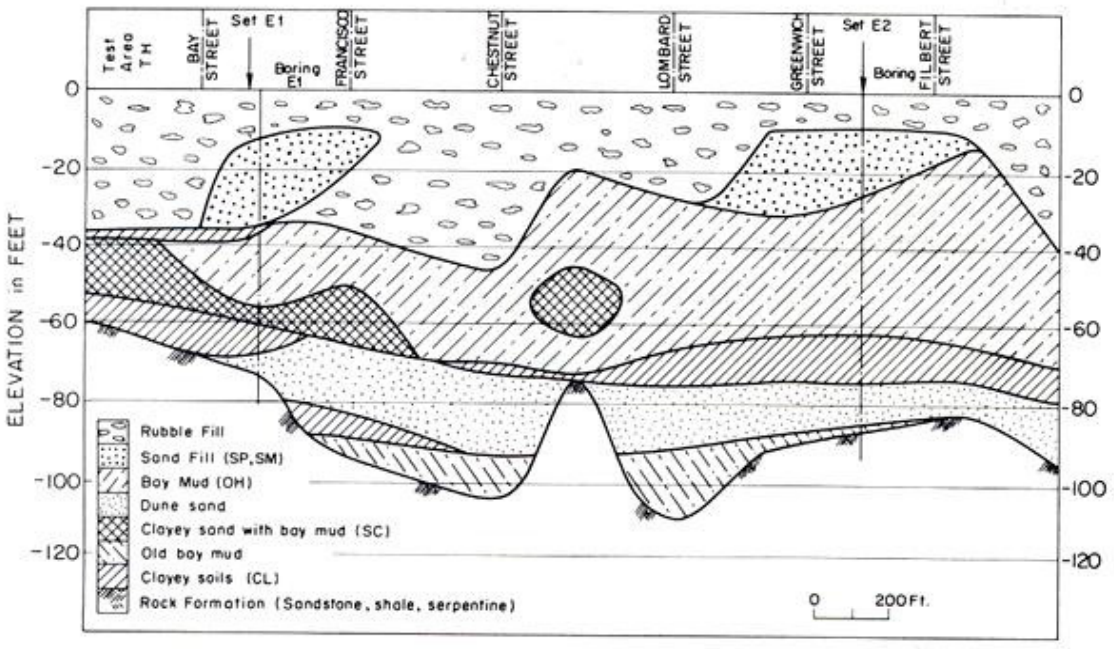

Figure 1: Idealized soil profile of Embarcadero Area in San Fransisco (Clough and Chameau, 1980).

Sheet piles (11 to 15 m long) were driven adjacent to borings E1 and E2 in Figure 1. Vibration attenuation in the horizontal and vertical directions was recorded by measuring peak horizontal and peak vertical acceleration at different distances from the piles. Settlement was also measured for both areas with distance from the piles, as shown in Figure 2.

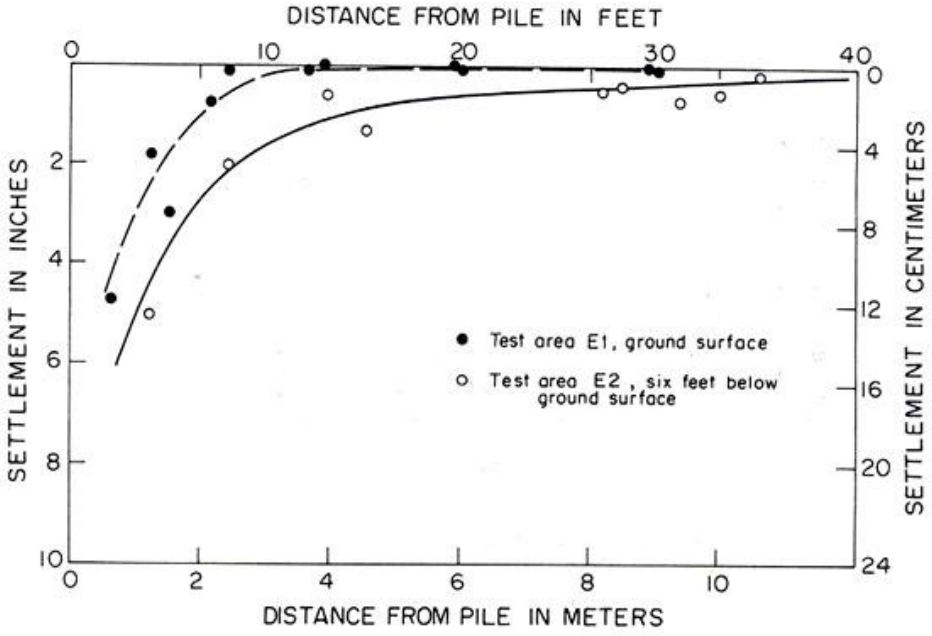

Figure 2: Settlement caused by sheetpile driving at E1 and E2 areas (Clough and Chameau, 1980).

Figure 2also shows that for the test area E1, the maximum settlement at the ground surface was 127 mm close to the pile and decreased to 0mm settlement at a distance of 3.6 m from the pile. For test area E2, settlement measured at points 1.83 m below ground surface was 0mm at a distance of 12m from the pile. Different soil densities were given as the reasons for this difference in that area E1 was denser than E2. This was supported by a standard penetration test and a cone penetration test used by the writers. The primary conclusions from the work were:

- The effects of vibratory pile driving attenuated rapidly with distance from the pile for all soils.
- Softer soils reduced accelerations more rapidly than denser soils apparently due to their greater damping capacity.

2.1.3 Picornell and del Monte (1982)

In northern Spain, H-piles were driven adjacent to the foundation of a steel mill resulting in settlements up to 254 mm.The building had a steel structure and the steel columns were anchored into concrete footings. Each footing was supported on two cast-in-place concrete piles. The soil was a granular deposit, loose to medium dense, with numerous limestone boulders. A significant number of mill piles were resting on these boulders. Static load tests up to the design loads indicated that the soil deposit was almost incompressible and not expected to settle, despite the low density. It was determined that vibrations during installation of the H-piles were responsible for the observed settlement.

2.1.4 Lacy and Gould (1985)

The authors present a review of factors influencing settlement from pile driving induced vibrations. It is a description of 9 case studies from Mueser Rutledge in the northeastern part of the United States. Five of these were case studies involving bearing piles and four involved trench sheeting. In addition, 10 cases studies from the literature were reviewed. The main factors of these cases are summarized in Tables 2 and 3. The major findings of their review are as follows:

- Settlement from pile driving in loose to medium dense sand can be caused by peak particle velocities lower than 51 mm/sec (2 in/sec), which is the normal criterion for vibration-induced damage. Vulnerable sites were damaged by measured ground surface peak particle velocities as low as 2.5 to 5.1 mm/sec (0.1-0.2 in/sec).
- Settlement was influenced by the following characteristics: Distance between the source of vibration and the affected structure, location of adjacent foundations and location of the water table.
- Damaging particle velocities, or accelerations, were much lower than values associated with modest seismic events. Pile driving operations created repeated small effects and eventually produced much greater settlement than that caused by earthquakes, with acceleration between 0.05 and 0.1 g.
- There is no simple method for estimating settlement on cohesionlesssoils based on peak velocity alone.
- There is no benefit in waiting between hammer blows.
- The case histories of sewer construction showed that it might be counterproductive to drive dewatering sheeting extra deep for hydraulic purposes, when the extraction of these sheeting piles may cause vibration, leading to settlement of the sewer.

The authors concluded that more research is needed to understand vibration-inducedsettlements. Note that in Tables 2 and 3, “distance pile to measurement” means the distance where the measurements were taken to the pile.

Table 2: Summary of Mueser Rutledge case histories in north-eastern United States (adapted from Lacy and Gould, 1985).

Location	Pile Type	Source of Vibration				Properties of Stratum Chiefly Involved					Remarks
		Hammer	Input Energy (ft./kips)	Distance Pile to Measure-ment (ft.)	Peak Particle Velocity (in./sec)	N (blows/ ft.)	D_{50} (mm)	D_{10} (mm)	U= D_{60}/D_{10}	Dr[1]	
Foley Square NYC	14HP73	Impact "Subsonic" Bodine- „Sonic"	26 - -	20 20 20	0.19 0.14 0.19	22-40 29	0.02 0.32	0.005 0.10	4 3	42-49 53-57	Building settled 3 in.
Lower Manhattan NYC	18 in open-end pipe	Vulcan 010	32	-	-	20-40	0.35	0.10	3	40-60	1.5 ft. settlement of street
West Brooklyn NYC	14 HP73	Vulcan 08	26	5-30	0.1	8-25	0.12	0.03	4	30-50 40-60[2]	Structure settled 3 in. as 40 piles were driven
South Brooklyn NYC	10.75 closed-end pipe	Vulcan 08	26	10-80	0.9-0.1	21-35	0.26	0.13	2	40	Structure settled 3 in. as 220 piles were driven
Lower Conn. River	12HP53	MKT10B3	13-20	3.5 c-c	-	20	0.42	0.10	4	40	Ground between piles settled 2.75 ft.
West Brooklyn NYC	Hoesch 134	ICE 812	4.0	3	-	27	0.12	0.03	4	48[2] 40-60	Building settled 2.4 in.
N. Syracuse NY	PZ-27	ICE 416	2.2	10-25	-	1	Sandy silt/silt/coarse to fine sand			25	Ramp settled 3 in. as sheeting removed
Syracuse NY	PZ-27	ICE 812	-	4 ft. from sewer	-	7	Fine sandy silt/ fine to coarse sand			30	Sewer settled 6 in. as sheeting removed
S. Queens	Hoesch 134	ICE 812	4.0	4 ft. from sewer	-	25	0.40	0.10	4	45	Sewer settled 3 in. as sheeting removed

Notes: 1) Relative density based on Bazarna 2) Relative density from actual measurement

Table 3:Summary of case histories from references (adapted from Lacy and Gould, 1985).

Driven Pile of Sheeting	Source of Vibration				Soil Data	Remarks
	Hammer	Input Energy (ft./kips)	Distance Pile to Measure-ment (ft.)	Peak Particle Velocity (in./sec)		
PZ (Belgium)	ICE 812	4	5 to 150	2 to 0.03	Loose fill with boulders soft clay and dense sand	18 Hz. D_r=35 to 65 percent. Plots of vertical strain versus ground acceleration for various values of D_r. Settlement up to 6 in.
PZ (Russian)	Drop	6.5	3 to 21	-	Medium sand	Measured peak particle accelerations. Settlement 0.2 in. Soil vibration 18 to 56 Hz.
24 in. Hollow concrete	Drop	20	-	-	Fill over sandy silt	Soil vibrating at 24 Hz. No measured settlement of water main.
Bearing piles	Percussive bored pile	-	10	-	-	Pile installation method avoided settlement from use of impact hammer.
Bearing piles	Impact hammer	-	Very close	-	-	Piles at varying distances were driven with different restrictions.
12 in. pipe and 14 in. shell	Vulcan OR	30	3.5 to 28 ft.	-	Sand fill; organic silt loose to medium dense sand (N=25); limestone compact sand.	Previously driven 60 to 80 ft. piles settled up to 7 in. Telltales showed vibration caused down drag loading the pile top to 35 tons. Required all piles be driven within 30 ft. before placing pile cap.
14 in. pipe	Link-belt 520 diesel	30	-	0.1 to 0.4	Rubble fill: 10 ft. to 30 ft. silty clay: 30 ft. + loose silty sand; stiff silty clay	Piles driven with mandrel. Peak particle velocity did not increase when driving resistance in lower stiff clay increased.
H-piles for trench	Diesel	-	-	-	Asphalt and fill/compact silty loam	Measured peak particle velocity was higher for 12 in. H-pile than for 14 in. H-pile.
Steel sheeting	Vibratory	-	110 12	0.09 0.2	Loose to medium dense sand	1/4 in. settlement 35 ft. from trench. 1/8 in. settlement 90 ft. from trench.
12 in. H-pile for trench	MKT 9B3	9	30	0.02	Loose to medium dense sand	Reported previous large settlement and extensive damage to buildings at another site with similar soils and same hammer steel sheeting. No settlement with H-pile.

2.1.5 Linehan, Longiow and Dowding (1992)

In this paper the authors describe the response and performance of a pressurized 300-psi natural gas pipeline in Northbrook, Illinois, adjacent to a construction site on which a pile foundation was being driven into the ground to widen an existing bridge. The sheet pile cofferdam walls for the bridge abutment were installed 2-4ft. from this 3.0ft. diameter steel pipeline. A plan view of the construction site can be seen in Figure 3. The pipeline had been routed beneath the existing bridge and ran parallel to a river. It had been buried 4 ft. below ground surface.Lateral and vertical settlements of the pipeline were measured by adapting land surveying methods. Ground and pipeline vibrations were measured with velocity transducers.

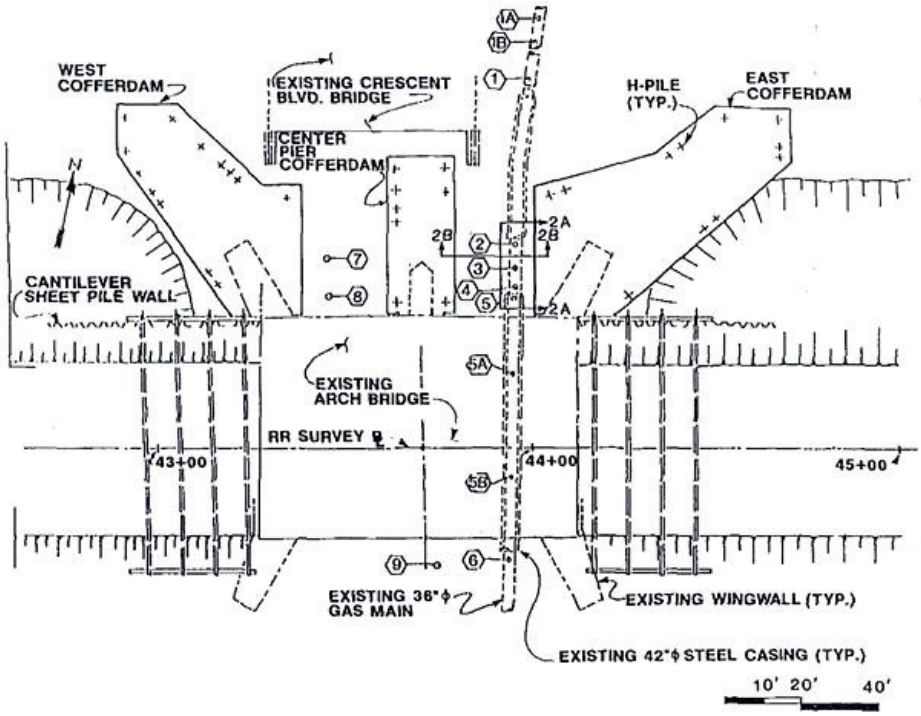

Figure 3: Plan view of construction site showing the pipeline running north-south and the cantilever sheet piles walls that caused settlements (Linehan, Longinow and Dowding, 1992).

Settlement and translation of the pipeline occurred during construction. The first significant movement occurred during driving piles for the west wall of the east cofferdam, a total of 0.5 inches were observed. Driving H-piles for the center pier produced an additional pipeline settlement of 0.75 inches and westward lateral movement of 1 inch. According to the authors, settlement and lateral movement of the pipeline were probably aggravated by the movement of the east wall of the center pier cofferdam during pile driving. It was reported that there was insufficient lateral support, therefore, additional whaler support beams were installed and the cofferdam was reinforced. The loose sand and soft silt river deposits had contributed to the horizontal movement of the pipeline during construction.The authors were more concerned about pipeline performance during construction than about actual soil behavior. Settlement and lateral movement of the pipeline were indicators that the soil structure had undergone some degree of deformation, but were not studied in detail.

2.1.6 Leathers (1994)

In this case study large settlements and lateral soil movementswere observed as a result of driving load-bearing piles into a medium-dense to dense sand layer in Boston, Massachusetts. Precast concretes piles, with an area of 355 mm², were driven to a depth of 29 to 39 m into a soil profile consisting of fill, silty gravel, and sand (see Figure 4).

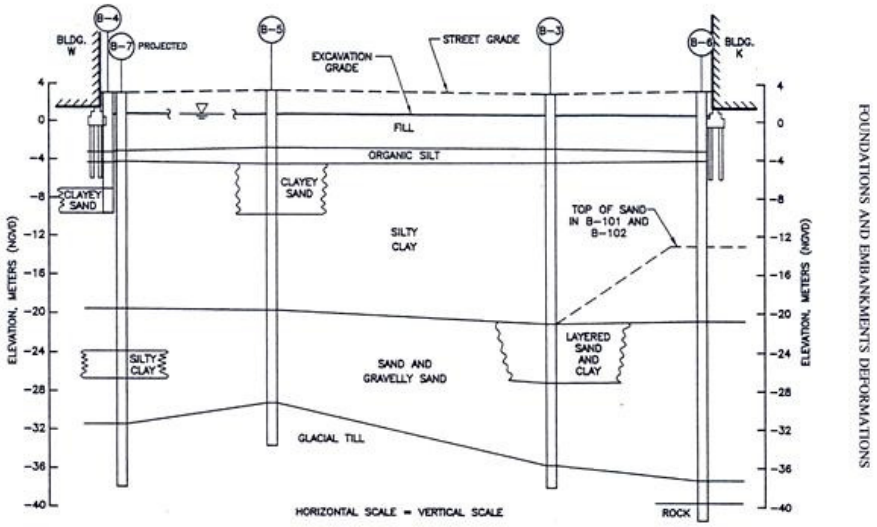

Figure 4: Subsurface profile through a site in Back Bay of Boston, Massachusetts (Leathers, 1994).

An ICE 640 diesel hammer was used to drive 180 piles. Settlement contours from the pile driving are shown in Figure 5. The settlements decreased with distance from the pile and the settlement gradient was higher below building K. The largest settlement of 54 mm occurred at the southwest corner of Building K. Please refer to Figure 4 for an illustration of the location where the piles were driven.

Settlement resulted from volumetric strain within the lower sand layer during driving. No volume changes occurred in the clay stratum. Densification in the medium dense sand was 1.7%, and in the dense sand it was 1.4%. The upper 9 m of sand showed the largest lateral soil movement.

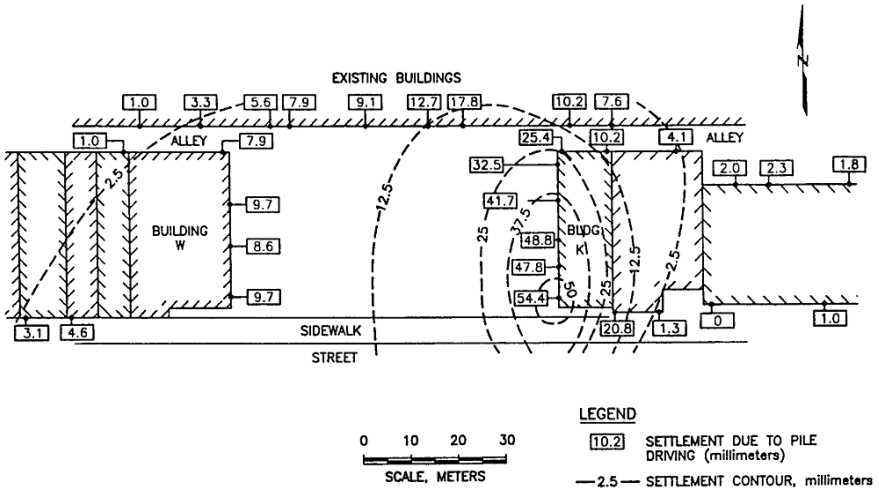

Figure 5: Settlement contours due to pile driving (Leathers, 1994).

Pore pressures in the sand and clay layers at this site were measured during the installation of two piles. The plan and profile locations of the piezometers are shown in Figure 6 (left). The piezometers were in-between the piles C-11-5 and C-13-1. Piezometer PZ-2A was installed in sand and PZ-2B in silty clay. In Figure 6 (right) the measured pore pressures during pile driving are shown.

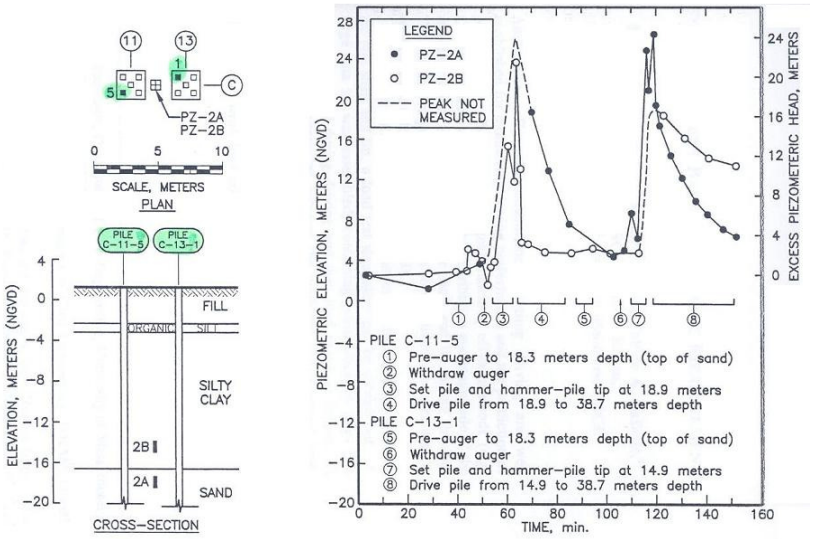

Figure 6: (Left) Plan and cross- section of piles C-11-5 and C-13-1 with the piezometers PZ-2A and PZ-2B. (Right) Pore pressures recorded during pile driving.(Leathers, 1994).

Piezometer PZ-2A showed only small changes in pore pressure during pre-augering of pile C-11-5 to 18.3 meters depth. As pile C-13-1 was lowered into the hole, a small spike and rapiddissipation of pore pressure occurred. At the start of pile driving, a quick build up in pore pressure was recorded with a maximum excess piezometric head of 24.4 m, or 239 kPa excess pore pressure. This large pore pressure increase resulted from prompt densification of the sand during driving.

Piezometer PZ-2B indicated a rapid increase in pore pressure, followed by rapid dissipation during the installation of pile C-11-5. During the alignment of C-13-1, the pile tip stopped in the clay about 3.4 m above the bottom of the pre-augered depth indicating that the hole had not been properly cleaned prior to pile installation. In addition, displacement of the clay during driving created an excess pore pressure that dissipated slowly after completion of driving. The excess piezometric head at the end of driving pile C-13-1 was 4 m in the sand and 10 m in the clay. Two days after driving these piles, the excess piezometric head in the clay had dissipated to 5.9 m.

2.1.7 Bradshaw, Miller and Baxter (2007)

This case history describes substantial movements of a sheet pile wall during construction of a braced excavation. The city of Providence, Rhode Island upgraded its sewer system with construction of a 4.8 km long, 7.92 m diameter underground tunnel. The tunnel was designed as a temporary sewer overflow. For the construction of a gate and screening structure for the tunnel, deep cuts were required into the ground consisting of non-plastic silt (Figure 7).

The underlying silt was identified as loose and susceptible to ground movement during construction. Prior to excavation, geotechnical instrumentation was installed (Figure 7). The instrumentation consisted of one monitoring well (OW-4), 3 inclinometers (INC-4, INC-5 and INC-10), and 2 multi-level vibrating wire piezometers (PZ-1 and PZ-2) installed below the bottom of the excavation.

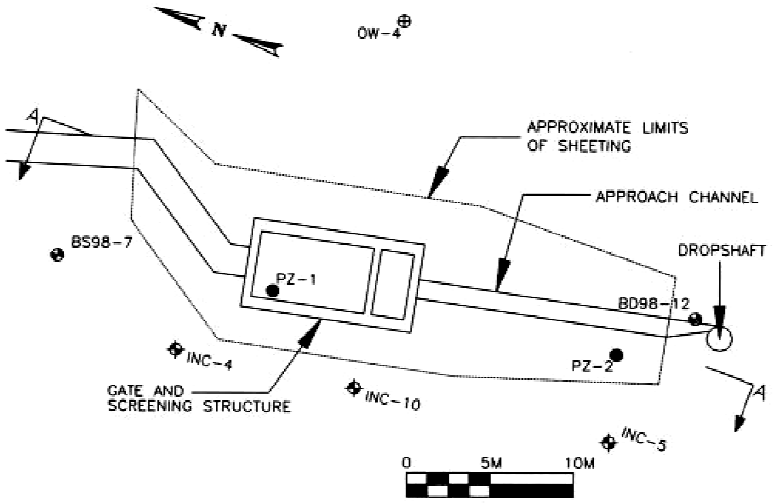

Figure 7: Site plan showing extent of excavation for gate and screening structure and locations of boring and geotechnical instrumentation (Bradshaw, Miller and Baxter 2007).

The braced excavation consisted of sheet piles with steel walers and struts driven to a depth of 16m below ground surface with a sump pump to a depth of 8 m for dewatering. A perforated lean concrete mat was installed at the bottom of the excavation. These perforations allowed 31 steel H-piles to be driven through the mat to support the new concrete gate and screen. The piles were driven with a vibratory hammer to a depth of 24m below the bottom of the excavation.

The sheet piles bulged during excavation; however, after installation of the mat no further bulging took place. During driving of the H-piles the sheet walls moved towards the interior of the excavation. The largest displacement was at a depth of 10 m below ground surface. At the same time, no vertical movement of the mat was observed.

Inclinometer data was recorded during construction and allowed the assessment of wall deformation. Data from the northernmost inclinometer (INC-4) is shown in Figure 8. Bulging of the wall caused by excavation is shown by the data points from 11/5/03 to 1/14/04. The lateral movements were larger than expected. Later installation of the lean concrete mat showed no additional lateral deformation, as shown by the data for the dates of 1/14/04 and 2/3/04. When pile driving began on 2/2/04, displacements were recorded towards the interior of the excavation.

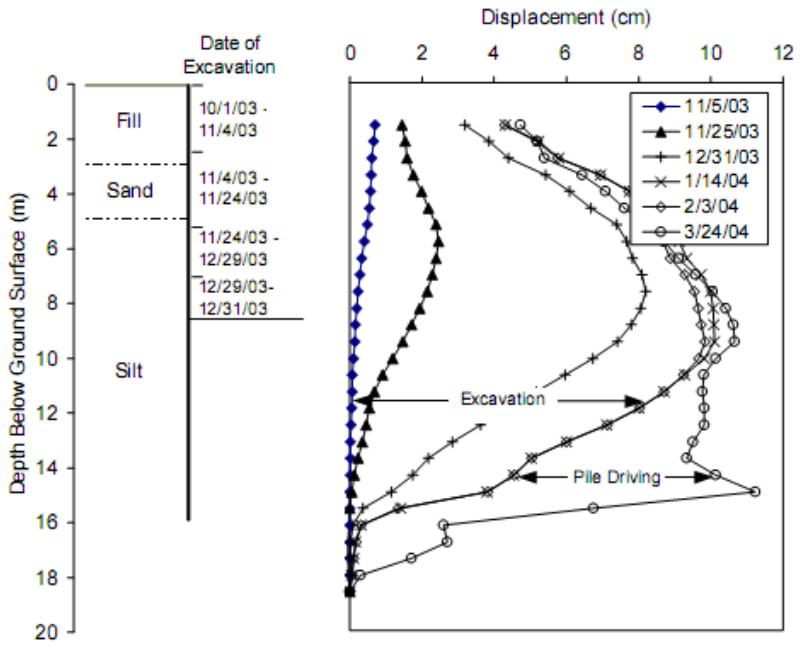

Figure 8: Inclinometer data from the northernmost inclinometer (INC-4) showing wall deformations during the construction (Bradshaw, Miller and Baxter 2007).

The authors speculated that two factors were at play to explain the displacements:

- The sump pump appeared to have eroded silt from beneath the mat, which may have created a gap beneath the mat.
- Vibration during pile driving in the silts layer may have been the cause of the lateral deformation. Shear waves generated by pile driving could have induced cyclic shear stresses resulting in pore fluid excitation. This excitation would yield a temporary reduction in effective stress, leading to a decrease of soil strength and stiffness. Later dissipation of this excess pore pressure would lead to soil densification and significant settlement.

Piezometric data was recorded and evaluated to assess if the pore fluid generation could be attributed to pile driving. The collected data was used to quantify the excess pore pressure generated during driving of individual piles.

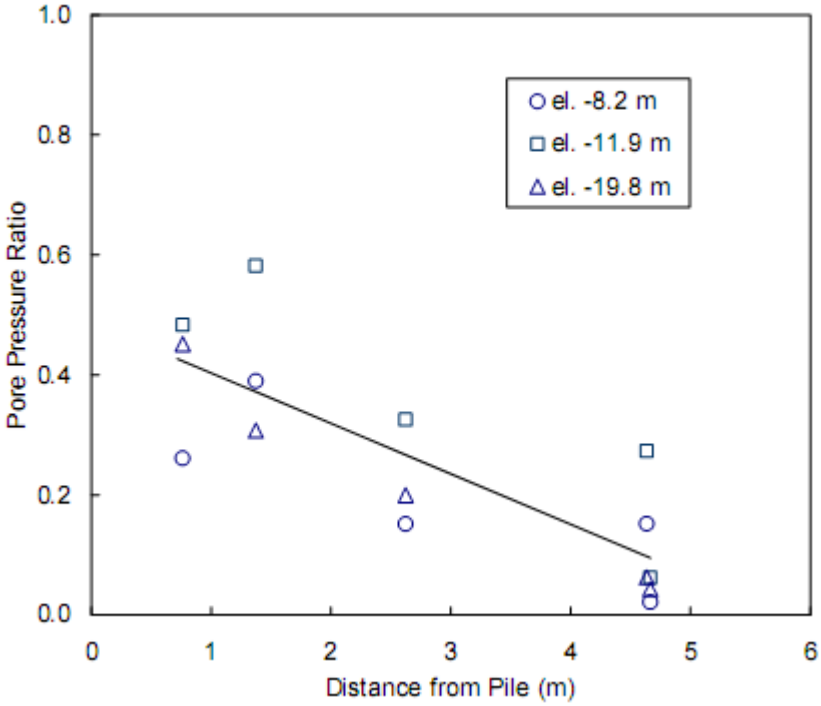

Figure 9: Excess pore pressure ratio calculated from piezometer data recorded during vibratory driving of H-piles (Bradshaw, Miller and Baxter 2007).

The pore pressure ratio (r_u), defined as the ratio of the excess pore pressure to initial vertical effective stress, was calculated as a function of radial distance from the pile (Figure 9). It can be observed from this figure that excess pore pressures were generated during pile driving and these pressures decreased with radial distance to zero within about 5 meters of the pile.

The main features of the case studies presented above are shown in Table 4.

Table 4: Comparison of the different cases studies

Reference	Source of Vibration	Type of Pilling	Ground Condition	Settlement	Excess pore pressure	Remarks
Dalmatov, Ershov and Kovalevsky	Drop Hammer	Sheet piles & hollow reinforced concrete	Fill over silty sand	Critical distance 7 and 8.2 m	-	Comparison of observed to critical accelerations
Clough and Chameau	Vibratory hammer	Sheet piles	Fill, bay mud, dense sand and clay	max. 127 mm	-	
Picornell and del Monte	Driving	H-piles	Granular soil on limestone boulders	25 mm building	-	
Lacey and Gould	Various Driving Techniques	End Bearing and Sheetpiles	Various	76 mm – 838 mm	-	Peak velocity not a good basis for settlement prediction
Linehan, Longiow and Dowding	Vibratory Hammer	Sheet piles	Dense sand and gravel	1.25 in. of pipeline	-	
Leathers	Diesel Hammer	Precast concrete piles	Fill, gavel, sand	54 mm of building	239 kPa excess pore pressure	
Bradshaw, Miller and Baxter	Vibratory Hammer	Sheet piles	Silt	-	Pore pressure ratio of 60%, liquefaction	11 cm lateral displacement of sheet piles

2.2 Methods for the Prediction of Settlement due to Pile Driving

Predicting the settlement of ground adjacent to pile driving has become of critical interest to civil engineers. This section presents an overview of various methods proposed in the literature for predicting settlement. However, the proposed methods are confined to sand to silty-sands, as there is no published research for predominately silty soils.

2.2.1 Massarsch (1992)

This paper presents an empirical approach for estimating the maximum settlement from pile driving based on ground acceleration and cone penetration resistance (Figure 10), which was developed from case studies of vibratory pile driving and vibratory soil compaction.

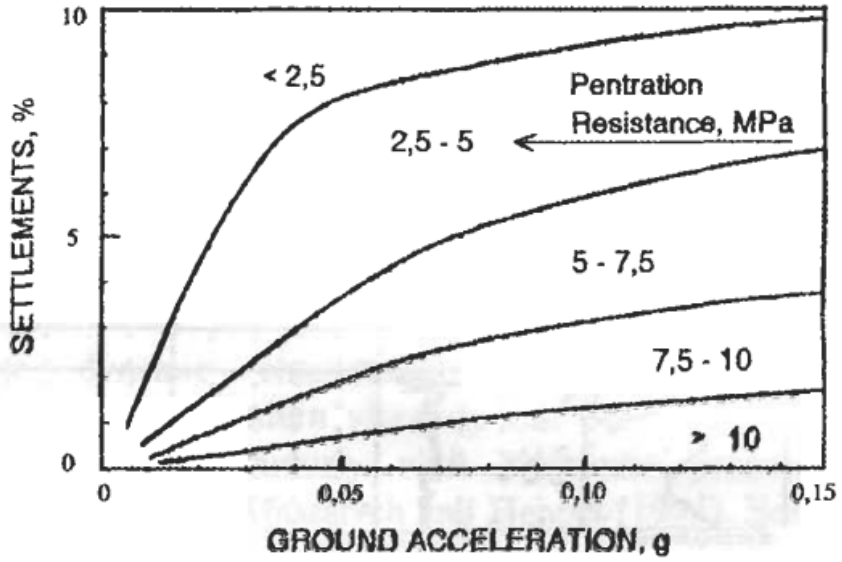

Figure 10: Settlement (as the percentage of the layer thickness) caused by vibratory pile driving and vibratory soil compaction (Massarsch, 1992).

Estimated settlements, reported as the percentage of the layer thickness, range from 10% for very loose sand and silt, to 1% for dense sand and gravel. However, there was no mention whether the corrected or uncorrected CPT measurements were used; nor was the duration of the vibratory accelerations considered (Meijers, 2007).

2.2.2 Massarsch (2000)

Massarsch also developed a quantitative evaluation of settlement due to surface vibration derived from dynamic and cyclic laboratory tests. In this methodology the volumetric strain (or settlement) is a function of shear strain amplitude. The shear strain amplitude $\Delta\gamma$ was derived from the vibration amplitude (particle velocity) υ and the shear wave velocity C_s, to

$$\Delta \gamma = \Delta \upsilon / C_s. \qquad (1)$$

For the variation of the vibration amplitude with depth the situation of Rayleigh waves was assumed. Settlement in loose sand due to ground vibration was estimated from this shear strain amplitude:

$$\Delta s = f_1 m_z \upsilon \Delta H / (R_s C_s) \qquad (2)$$

where

- Δs settlement in that layer,
- f_1 empirical parameter relating the plastic vertical strain to the shear strain amplitude (cp. Figure 11),

m_z parameter relating the vibration amplitude at depth z to the vibration amplitude at ground level (cp. Figure 12),
υ vibration amplitude (velocity amplitude) at ground level,
ΔH thickness of considered layer,
R_s ratio between Rayleigh wave velocity and shear wave velocity (0.93),
C_s shear wave velocity.

Massarsch re-analyzed data published by Youd (1972) and Seed and Silver (1972) to study the relationship between vertical strain ε_z and shear strain γ as a function of shear strain amplitude and for different numbers of load cycles. The results are shown in Figure 11. The parameter f_1 is the ratio between the vertical strain and the shear strain amplitude. It is a function of the shear strain amplitude and the number of equivalent cycles.

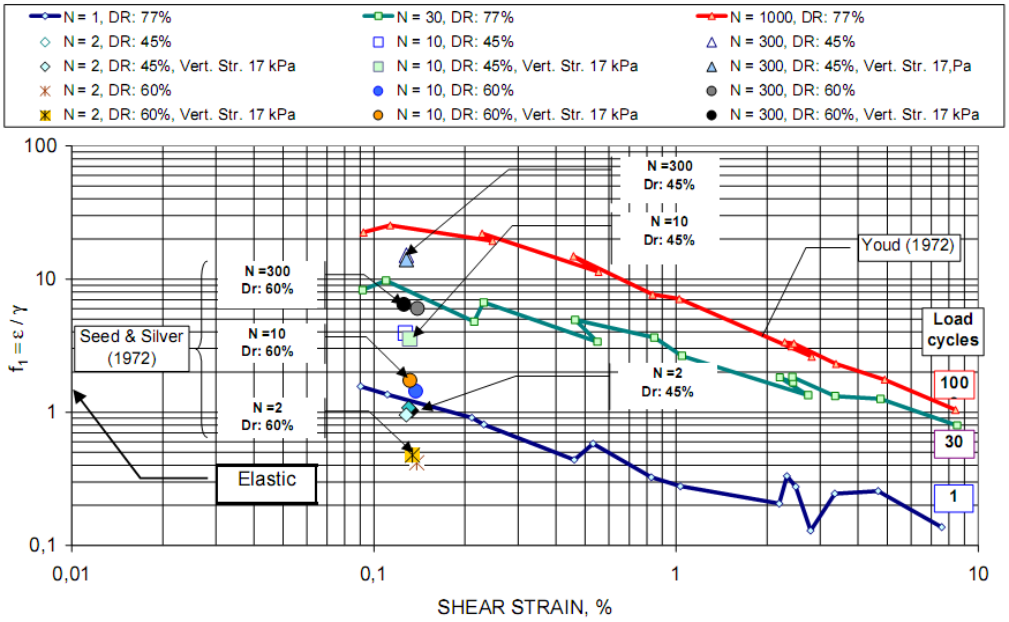

Figure 11: Shear strain factor f_1 as function of shear strain for different values of load cycles (N) and relative density (DR), data Seed and Silver (1972) and Youd (1972) (Massarsch, 2000).

An important question in determining settlements caused by the passage of waves is the estimation of shear strain variation with depth. Mohamed and Dobry (1987) developed charts for assessing the variation of shear strain in terms of peak particle velocity. Figure 12 shows the variation of the shear strain factor m_z with dimensionless depth z/L for use with vertical peak particle velocity. The influence of Poisson's ratio is relatively small for cohesionless soils, so for most practical purposes a simplified, linear relationship m_z= 0.9 – 0.6 z/L can be used. With this relationship, the variation of shear strain amplitude based on the measurement of the vertical vibration amplitude at the ground surface could be estimated.

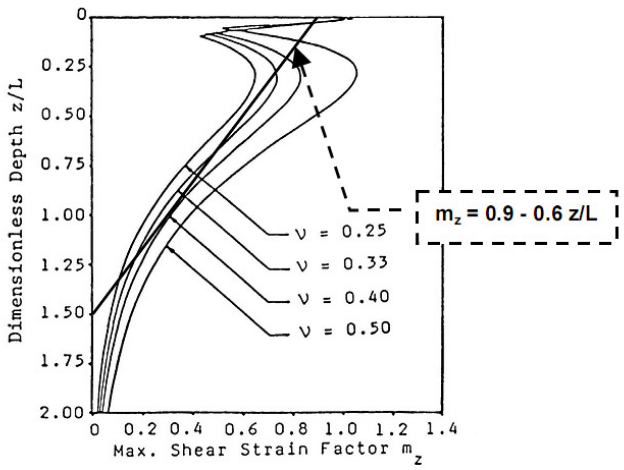

Figure 12: Shear strain factor m_z for use with vertical peak particle velocity, after Mohamed and Dobry (1987), with indication of simplified relationship (Massarsch,2000).

The Massarsch method only used 300 load cycles as loading pattern (Figure 11). This is a relatively small number in comparison to the number of cycles that occur when a pile is driven.In addition, the method assumes the presence of Rayleigh waves, which are only in a far-field situation. This is at a distance of 1.5 or 2 times the wavelength. The largest settlement is, however, to be expected closest to the pile, in the near field (Meijers, 2007).

2.2.3 Massarsch (2004)

The most current method, proposed by Massarsch is a simple engineering approach to estimate settlement adjacent to a single pile in a homogeneous sand deposit. There are two primary assumptions in this analysis: (1) there is significant densification within a zone around the pile equal to three times the pile diameter (3D) and (2) densification is manifested at the ground surface as a settlement to a distance of 3D + L/2(Figure 13).

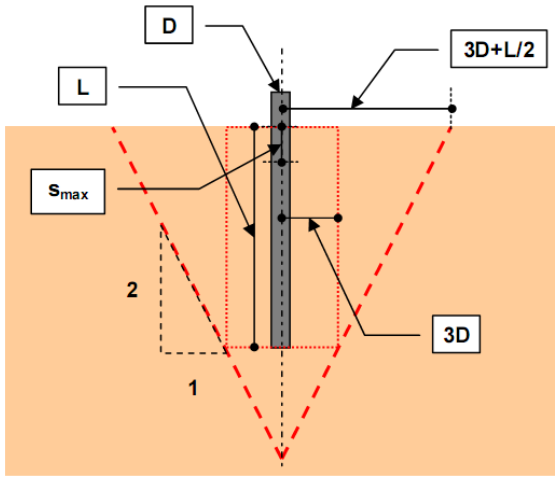

Figure 13: Zone of densification and resulting settlement as predicted by the simplified method of estimating settlements adjacent to a single pile in a homogeneous sand deposit (Massarsch, 2004).

The maximum settlement, s_{max} and the average settlement, $s_{avg}$are estimated in this approach using the following equations

$$s_{max} = \alpha\ (L+ 6D)\ ; \qquad s_{avg} = \frac{\alpha\ (L+ 6D)}{3} \tag{3}$$

where

L length of the pile,
D diameter of the pile,
α empiricalcompression factor

Table 5: Compression factor for different ground conditions and driving energies (from Massarsch(2004))

	Compression factor, α		
Driving Energy	**Low**	**Average**	**High**
Very loose	0.02	0.03	0.04
Loose	0.01	0.02	0.03
Medium	0.005	0.01	0.02
Dense	0.00	0.005	0.01
Very dense	0.00	0.00	0.005

Driving energy is a subjective measure that depends on the method of pile installation, pile type and soil stratification.

2.2.4 Drabkin, Lacy and Kim (1996)

Construction and maintenance of buildings and roads, such as pile-driving activities, generate vibrations in the nearby structures that might lead to undesirable settlements or structural damage. Drabkin et al (1996) develop a method to predict in situ settlement of sands caused by pile driving or vehicular traffic with an empirical model that takes into account vibration characteristics (amplitude, frequency, number of cycles), source of vibration, distance to that source, soil parameters (attenuation characteristics, grain size distribution, moisture content, density) and state of stresses in the soil layers vulnerable to vibrations. The method was developed from 27 cyclic triaxial tests on dry and moist sand. In these tests a triaxial cell was attached to a vibratory frame and vertically vibrated at a frequency of 60 Hz. Vertical deformation of the sample was measured. The formula to estimate settlement Y (mm) is as follows:

$$\ln Y = 2.27 + 1.19\ x_1 - 0.71\ x_1^2 + 0.49\ x_2 - 0.68\ x_2^2 - 0.80\ x_3 + 1.09\ x_3^2 - 0.46$$
$$x_4 + 0.06\ x_4^2 + 0.45\ x_5 - 0.38\ x_5^2 - 0.19\ x_6 - 0.10\ x_7. \tag{4}$$

Table 6 shows the range of values for each variable in Eq. (4).The vibration amplitude (x_1) would be measured on a site using a seismograph; the deviator stress (x_2) and the confining stress (x_3) are taken from the mid-point of the vulnerable layer in the field. The other parameters, such as sand type, moisture content, relative density, and the number of vibration cycles are obtained from field records.

For example, for construction operations, traffic, pile driving, and dynamic compaction, vibration amplitudes range from 2.5 mm/sec to 25 mm/sec (Drabkin et al., 1996). For proper settlement assessment, vibration amplitudes should be monitored both at the ground surface and within the ground.

Table 6: Factors, coding and tested ranges used to estimate settlement (adapted from Drabkin, Lacy and Kim, 1996).

Designation	Factor	Coding	Tested Ranges	[Unit]
X_1	Vibration amplitude	$X_1 = -1+(\upsilon-0.1)/0.3$	2.5-18 mm/s	Inch/sec
X_2	Deviator stress	$X_2 = -1+(s-2)/6.5$	14-104 kPa	Psi
X_3	Confining pressure	$X_3 = -1+(p-10)/10$	69-207 kPa	Psi
X_4	Sand mixture	$X_4 = -1/0/1$	Coarse (d_{50}=1.7mm) Medium (d_{50}=0.7mm) fine (d_{50}=0.5mm)	-
X_5	Number of vibration cycles	$X_5 = -1+ (N-60) /26,997$	N=60-500,000	-
X_6	Moisture content	$X_6 = -1/2$	Dry, saturated	-
X_7	Initial relative density	$X_7 = -1/2$	Loose, medium dense	-

Legend:
- υ : vibration amplitude
- s: deviator stress
- p: confining pressure
- N: number of cycles

This method was applied to evaluate vibration-induced settlements due to pile driving activities of different projects such as:

- Back Bay site in Boston, MA – densification of sand layers during pile driving in the middle of a block of existing.
- Cedar Creek site in Wantagh, New York – evaluation of vibration effects on settlement to permit the use of a vibratory hammer to drive sheeting near existing structures and the construction of several effluent tanks.
- Lesaka Site, Spain – pile driving induced settlement of a pier foundation.
- Tri-Beca site in Manhattan, NYC – pile driving induced settlement in a 52 story residential building that was to be constructed near two other existing buildings.

Results showed good agreement between calculated and observed settlements.

2.2.5 Bement and Selby (1997)

Bement and Selby also developed an empirical method for estimating vibration-induced settlements from a series of laboratory tests. In situ conditions of nine different granular soils (sands to sandy fine-to-medium gravels) were recreated in a laboratory using a Rowe cell, which enables soil samples to consolidate under static stress conditions. After consolidation, samples were subjected to different vertical vibrations at increments of controlled acceleration, under conditions of free drainage and constant confining stress.

Using this method, Bement and Selby were able to predict settlement based on acceleration, total vertical stress, and grain size distribution of the soil with the following equation:

$$S_v = \frac{2.8\ln(D_c)a^2}{D_r\sigma_v} \; ; \quad D_c = \frac{D_{90}}{D_{60}D_{30}} \qquad (5)$$

where

S_v	settlement in %,
a	acceleration amplitude [g]
D_c	grain size distribution [mm-1]
D_r	relative density,
D_{60}	particle with 60% passing;
D_{90}	particle with 90% passing
σ_v	vertical stress [kPa]

Equation (5) was developedfrom a series of tests with an overburden stress of 10 to 100 kPa, acceleration levels between 0.02 *g* to 1.0 *g*(typically sinusoidal vibration for soils within 2-20 m of a pile driven with a vibratory hammer) and frequencies of 25 to 40 Hz. They noted that if acceleration values exceeded 2g the soil would liquefy and the following equation (6) would apply:

$$S_v = \frac{4(\ln(D_c)+0.7)\ln(a))}{0.01(\sigma_v)+0.75(1-D_r)}. \qquad (6)$$

The primary application for this concept is to enable predictions or estimations of ground settlement adjacent to pile driving activities. In this approach it is assumed that you know the soil profile in question and the ground surface vibrations. If the ground surface vibrations are unknown, it is suggested that they are estimated using Attewell et al. (1992).

2.2.6 Lukas and Gill (1992)

The authors present a theoretical approach to predict settlement from pile driving. The theoretical estimate of ground settlement from vibration acceleration and number of cycles during pile driving was based on procedures described by Seed and Silver (1969 and 1972), Silver and Seed (1971), and Lee and Albasia (1974) for settlement induced by earthquakes. Lukas and Gill's procedure mimics the methodology for calculating settlement during earthquakes as follows:

(1) Divide the soil into different thin layers of equal relative density.
(2) Compute overburden pressure in mid-depth of each layer.
(3) Determine the shear modulus - G - from each layer (from Seed and Silver (1971))

$$G = 1000K_m\sigma'^{m}_{v} \text{[pounds per square foot]} \qquad (7)$$

where

σ'_v	vertical confining pressure,

m exponent between 0.6 and 0.7 and
K empirical coefficient for the shear strain

(4) Find shear strain amplitude in each layer from

$$\tau = \gamma * h * a_{max} * r_d \quad (8)$$

where

a_{max} *acceleration as fraction of gravity,*
$\gamma * h$ overburden pressure,
r_d depth factor which varies from 1.0 at surface, to 0.9 at 9.6 m depth and reduces parabolic to 0.65 at 20 m depth.

(5) Determine the average shear strain amplitude from

$$\Delta\tau = 0.65 * \Delta\tau_{max} \quad (9)$$

(6) Calculate the shear strain

$$\Delta\gamma = \Delta\tau_{avg} / G \quad (10)$$

(7) Obtain the vertical, or volumetric, strain for each layer from published data. There is a relationship between the shear stain amplitude, the number of loading cycles and the volumetric strain. An example of this relationship for silica sand is provided by Seed and Silver (1972) on Figure 14.

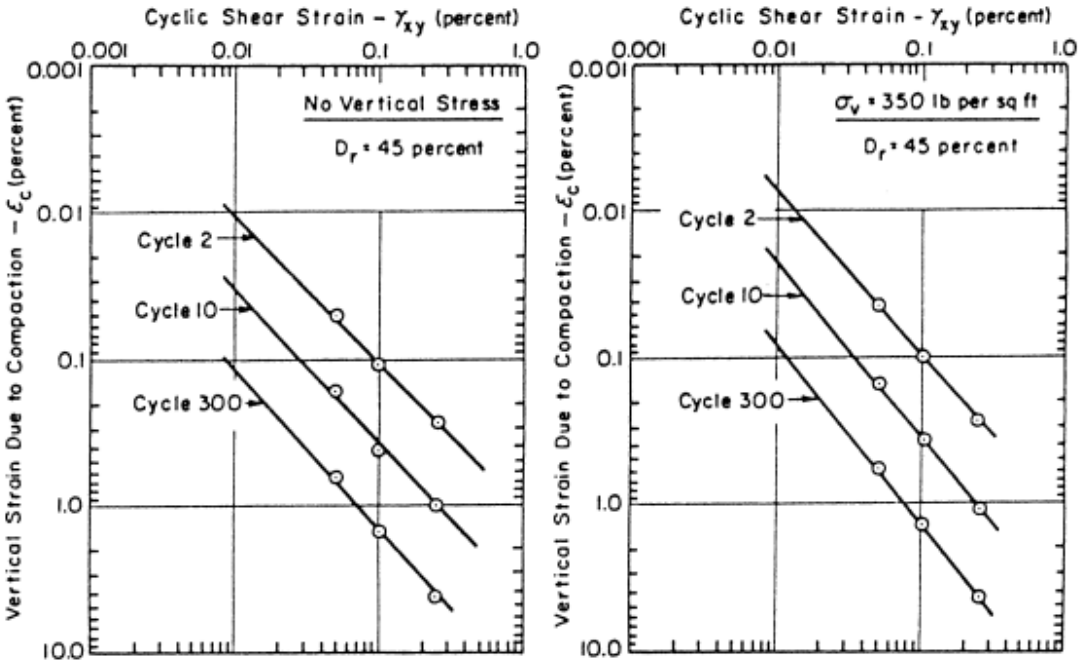

Figure 14: Vertical settlement - shear strain relationship for silica sand, Seed and Silver (1972).

(8) Compute settlement of each layer from the volumetric strain.

2.2.7 Comparison of Published Methods

Meijers (2007) performed a detailed review of published methods for estimating settlements due to pile driving and vibrations. A comparison of the methods by Meijers is shown in Table 7.

Table 7: Comparison of methods for estimating vibration-induced settlements. Adapted from Meijers (2007).

Method	Input parameter	Number of cycles in-corporated	Excess pore pressure generation	Density of sand considered	Type of piling	Remarks
Massarsch (1992)	Acceleration	No	No	Yes	Vibratory pile driving	
Massarsch (2000)	Shear strain amplitude	Yes	No	Partly (45 and 60%)	Not mentioned	
Massarsch (2004)	None	No	No	Yes	Not mentioned	
Drabkin et al. (1996)	Velocity amplitude	Yes	No	Yes	Not mentioned	
Bement and Selby (1997)	Acceleration	No	No	No	Vibratory sheet piling	Grain size distribution is accounted for
Lukas and Gill (1992)	Shear amplitude	Yes	No	Yes	Not mentioned	

Four major conclusions were made from the comparison of the methods shown in Table 7:

- None of the methods included the effects of pore pressures on settlement. Meijers pointed out that the effects of spreading and pile volume are neglected in the prediction methods, and that none of them examine pore pressure during pile driving.In cases where pore pressures cannot be neglected these methods are of little value.
- If vibration frequency is taken into account, this will have an effect on acceleration amplitude, but not on other driving forces. Meijers showed that the different approaches used acceleration, velocity amplitude or shear strain amplitude as the driving forces for settlement. If the vibrations are mainly a result of shear waves, the relation between the driving forces is the following:

$$\Delta\tau = G\Delta\gamma = G\frac{\Delta v}{C_s} = G\frac{\Delta a}{2\pi f C_s}. \qquad (11)$$

where

$\Delta\tau$ shear stress amplitude,
$\Delta\gamma$ shear strain amplitude,
Δv velocity amplitude,
Δa acceleration amplitude,
G shear modulus,
C_s shear wave velocity ($C_s = \sqrt{\rho\ /\ G}$),
f frequency.

- The driving forces are proportional to each other, but only acceleration amplitude is frequency dependent.
- None of the methods presented above modeled actual pile-soil interaction during pile driving, and its effect on densification in a completely realistic manner.
- From the analysis of the six methods, and Meijers comparative table, it is clear that no single method is appropriate for application as a general method to predict settlement, as a result of pile driving.
- Furthermore, none of these models examine settlement in silt.

3. Experimental Methods

3.1 Background

In this study, an experimental testing program was developed involving undrained cyclic triaxial tests on samples of Providence silt. The objective of this testing program was to measure volumetric changes caused by dissipation of excess pore pressures following dynamic loading. The results of these tests will be incorporated into a larger laboratory testing program to develop and validate a constitutive model to predict settlement of silts due to pile driving activities.

Cyclic triaxial tests were pioneered by Seed and Lee (1966), Castro (1975), and others to study liquefaction of cohesionless soils. In 1976, Silver et al. provided a standard for cyclic triaxial testing of sand so that laboratories could create comparable results under similar conditions.

The aim of this methodology was to measure volumetric changes in silts *prior* to liquefaction. In this study, cyclic triaxial tests were stopped at a specified pore pressure ratio was achieved (prior to liquefaction). Drainage was then allowed and the volumetric strain was measured. This approach was used by Ishihara and Yoshimine (1992) and Lee and Albaisa(1974) to estimate volume changes in sand deposits following earthquakes. However, this approach has not been applied to silts.

Lee and Albaisa (1974) investigated the effects of cyclic loading, via cyclic direct simple shear testing, of saturated sands to illustrate the range of volumetric strain which may be expected to follow from dissipation of excess pore pressures developed during cyclic loading. In their studies, the effect of relative density for Monterey sand on volumetric strain was analyzed. The results are shown in Figure 15.

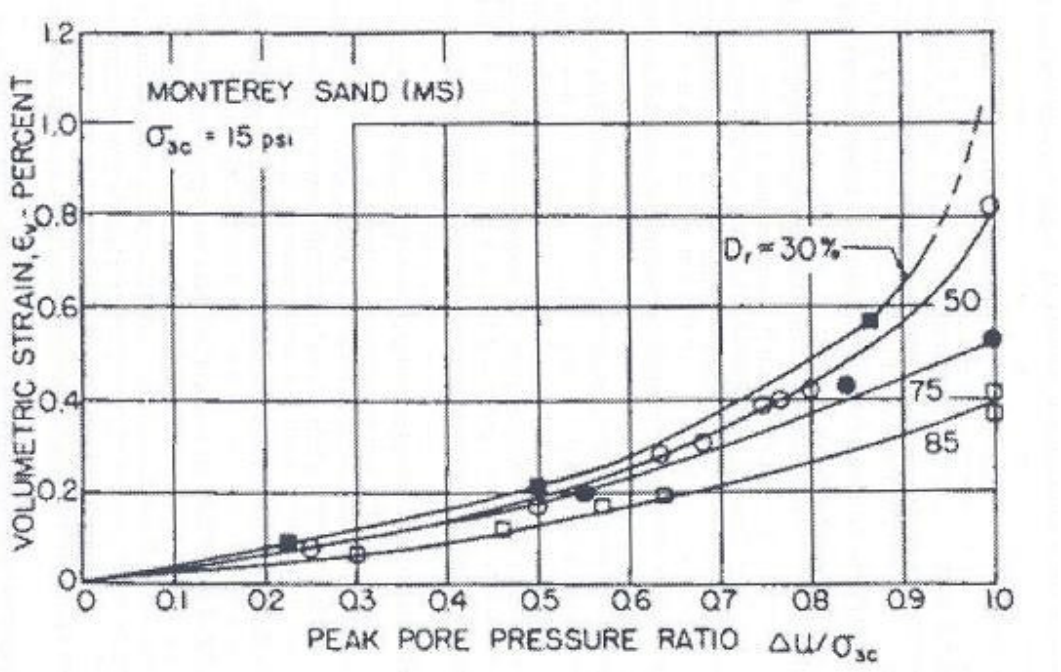

Figure 15: Effect of relative density on reconsolidation volumetric strain for Monterey sand (Lee and Albaisa, 1974).

They concluded that the amount of reconsolidation volumetric strain for non-liquefaction conditions increased with increasing grain size of soil, decreasing relative density, and increasing excess pore pressure generated during the undrained cyclic loading. In addition, the volumetric strain was almost independent of how this excess pore pressure was generated, even under static conditions. If liquefaction was observed, the resulting volumetric strain was likely to be less than 1%.

Ishihara and Yoshimine (1992) modified the work of Lee and Albaisa (1974) by terminating the undrained cyclic loading phase of a cyclic triaxial test at a selected level of pore pressure within a sample. The sample was then isotropically consolidated and the volumetric strain calculated. The volumetric strain resulting from dissipation of pore water pressures was correlated to the density of sand and a factor of safety against liquefaction. For a given factor of safety and density in each layer of a sand deposit, the volumetric strain was calculated and the volume changes throughout the depth were integrated. Thus, it became possible to estimate the amount of settlements on the ground surface produced by shaking during earthquakes.

3.2 Test Equipment

The equipment used to perform the cyclic triaxial tests was manufactured by the Geocomp™ Corporation of Boxborough, Massachusetts. Geocomp equipment provides its own software and data acquisition, for fully automated testing with the machine. The equipment (see Figure 16) consisted of:

- One LoadTrac II load frame,

- Two FlowTrac II flow pumps,
- One load cell,
- One linear variable displacement transducer (LVDT),
- One hydraulic actuator for applying the cyclic load,
- Two 200 psi pressure transducers.

A picture of the equipment is shown in Figure 16.

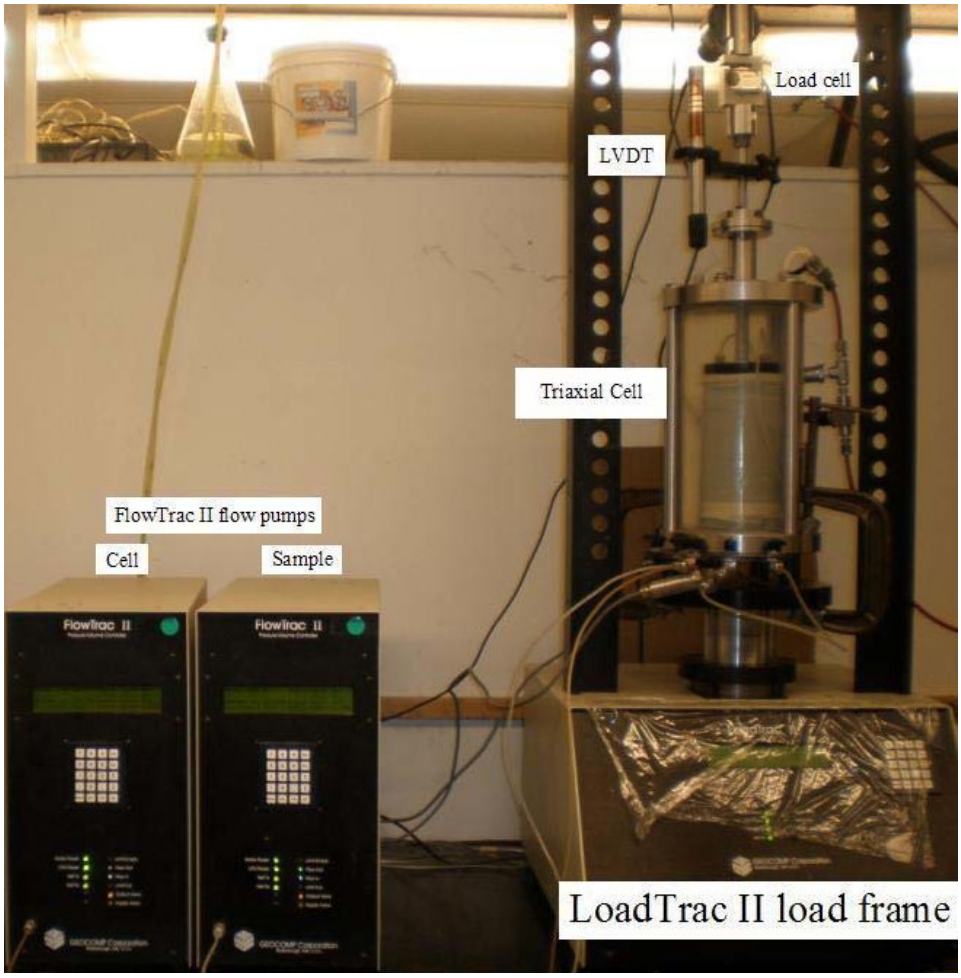

Figure 16:LoadTrac II load frame, triaxial cell and hydraulic actuator with the Flow Track II pumps.

3.3 Cyclic Triaxial Testing Procedure

Isotropically consolidated, cyclic undrained triaxial tests were performed on samples of reconstituted silts. Each sample was saturated by first flushing with CO_2, then inundation with de-aired water, and application of backpressure until a B-value of 0.97 was achieved. All samples were consolidated to 100 kPa prior to shear.

Samples were prepared using a Modified Moist Tamping Method (MMT) developed by Bradshaw and Baxter (2007). This method is based on Ladd's (1987) undercompaction approach. Unlike Ladd, who used different layer heights and keeping energy constant, the MMT method changes the fall height of the compaction weight for each layer to achieve a uniform density throughout the sample. The equipment consisted of a 5-cm diameter acrylic piston. A metal rod was attached to the piston. At a height greater than 14.2 cm above the piston, a stopper was fixed to the rod. A 900 gram drop hammer was guided by the rod and stopped by the stopper. An adjustable stopper was placed on top to control the fall height. The samples were prepared in a 7.2-cm triaxial split mold. The silt was installed in 8 layers, with each layer being tamped 25 times. The silt was mixed to a water content of 18%, which was the optimum water content determined in a modified Proctor Test (ASTM D-1557).

Samples were sheared undrained at different cyclic stress ratios (CSR) which is the applied cyclic shear stress divided by the effective confining stress ($\sigma_d/2\sigma'_c$). There are several failure criteria that have been used in cyclic triaxial testing. One of the most common is when the pore pressure ratio ($r_u=\Delta u/\sigma'_c$) reaches unity. When this occurs, the excess pore pressure is equal to effective confining stress, the soil has lost all its strength, and liquefaction has occurred. For the purpose of this study, the term liquefaction refers to the conditions of excess pore pressure ratios close to 1.0, which would facilitate large subsequent deformations under an applied shear stress.For fine grained soils such as the Providence silts, non-uniform pore pressures may develop during loading due to their low permeability, and the measured pore pressures at the end of the samples may be lower than the actual values along the failure plane within the samples (Zhou et al. 1995, Bradshaw 2006). In these cases, r_u of unity may not be an appropriate failure criterion, and a limiting strain criterion is often adopted. Figure 17 shows the definition of double-amplitude (DA) strain in a cyclic test, which isotropically, used as alternate failure criteria (e.g. 1%, 5% or 10% DA strain). For purposes of this investigation, a sample is considered "at failure" when the DA strain is equal to 5%.

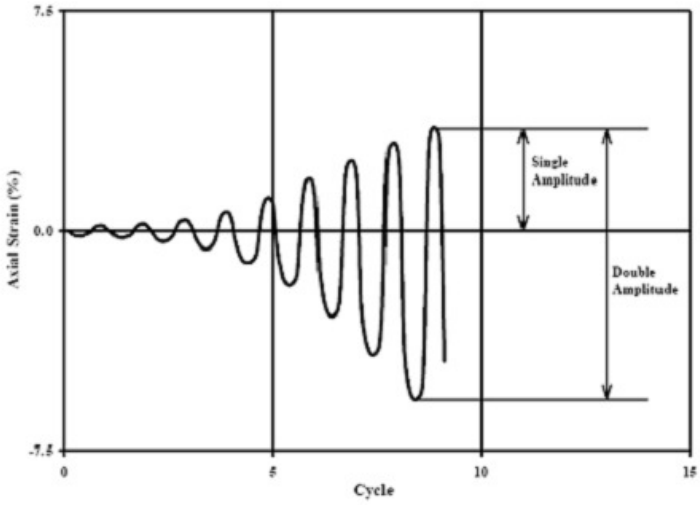

Figure 17: Definition of Double Amplitude (DA) strain (Polito, 1999).

3.4 Properties of the Silt Tested

To assess the liquefaction potential of Rhode Island silt, Bradshaw (2006) collected silt samples from two sites in the Providence area. The silt from Wellington Avenue was obtained from auger spoils produced during the installation of drilled shafts. Silt samples from the Olneyville neighborhood of Providence were obtained by in situ block sampling. These two materials were blended together and the geotechnical properties determined (Table 8). For comparison, Table 8 also includes the data from Bradshaw and Baxter (2007).

The specific gravity,G_s, was determined in accordance with ASTM D854. The minimum void ratio was determined from a modified compaction test (ASTM D 1557). Bradshaw (2006) found that the silt exhibited unreasonably high bulking when dry samples were utilized for the determination of the maximum void ratio in accordance with ASTM D 4254, so Bradshaw obtained maximum void ratios by allowing a slurry to settle out in a graduated cylinder. The same procedure was used for this study.

Table 8: Properties of silt used in this study

Soil	Specific gravity, G_s	Maximum void ratio	Minimum void ratio	D_{50} (mm)
Blended Silt	2.75	1.17	0.58	0.018
Wellington Ave. Silt[1]	2.78	1.11	0.57	-
Olneyville Silt[1]	2.71	1.22	0.61	-

(1) From Bradshaw and Baxter, 2007

The grain size distribution of silt used in this study is shown in Figure 18. The silt is classified as a ML according to the Unified Soil Classification System. Approximately 95% of the sample is silt or clay-sized particles. The soil is non-plastic. The grain size distribution was obtained using a Mastersizer 2000 sedigraph manufactured by Malvern Instruments.

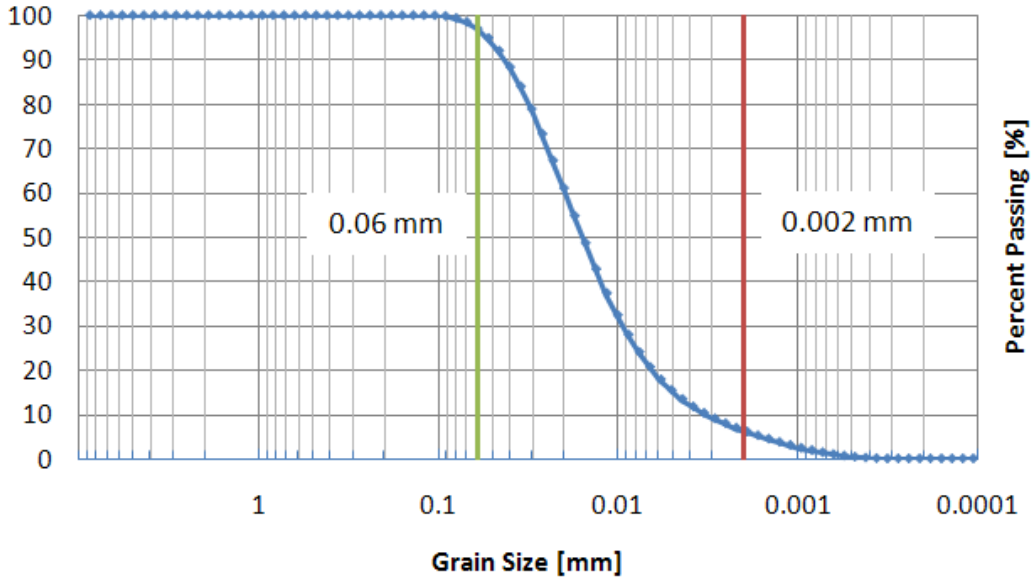

Figure 18: Grain size distribution of silt used in this study

3.5 Testing Matrix

The testing matrix for this study can be found in Table 9. Nine tests were performed on silt for this study. All tests were performed to study the volume change behavior of silt following cyclic loading. The first three tests were executed to study the effects of different cyclic stress ratio (CSR) on samples with the same initial density. Tests 1-4 were loaded until liquefaction occurred in the sample. The tests were manually stopped after the samples were completely liquefied. In tests 5 and 6 the samples were cyclic loaded to a pore pressure ratio smaller than 1, and then manually stopped. In order to develop a more efficient testing program, samples 7-9 were retested immediately after pore pressure build-up and reconsolidation stage. The aim was to simulate field conditions where cyclic loading could be stopped and restarted, allowing the soil to dissipate pore pressure and increase density.

The samples were prepared with initial relative densities varying from 41 % to 64 %. This band of relative density was chosen in order to study the effect of relative density on the volume change behavior of the silts following cyclic loading. The CSR varied from 0.08 to 0.14. The loading frequency for all the tests was kept constant at 0.5 Hz. This frequency was chosen over the standard 1 Hz to allow for more time for excess pore pressures to equilibrate within the sample during loading.

Table 9: Testing matrix for this study on silt samples

Test Number	Test Name	Initial e	Initial D_R	B-Value	Target CSR	F [Hz]	Abort criterion
1	CYC-09-20	0.82	59	0.97	0.12	0.5	A
2	CYC-09-22	0.84	56	0.98	0.1	0.5	A
3	CYC-09-23	0.83	57	0.98	0.08	0.5	A
4	CYC-09-26	0.93	41	0.97	0.12	0.5	A
5	CYC-09-27	0.91	45	0.97	0.1	0.5	Ae
6	CYC-09-28	0.86	53	0.97	0.1	0.5	Ae
7	CYC-09-19	0.88	49	0.97	0.12	0.5	N
	CYC-09-19b				0.12	0.5	N
8	CYC-09-21	0.81	61	0.97	0.12	0.5	N
	CYC-09-21b				0.12	0.5	N
	CYC-09-21c				0.12	0.5	N
9	CYC-09-24	0.79	64	0.97	0.14	0.5	N
	CYC-09-24b				0.14	0.5	N
	CYC-09-24c				0.14	0.5	N

Legend:
- e : Void Ratio
- D_R : Relative Density
- CSR : Cyclic Stress Ratio
- F : Frequency

Abort criterion:
- A : **A**bort manually after the sample was completely liquefied
- Ae : **A**bort manually **e**arlier than liquefaction (r_u<1)
- N : Abort after a pre-determined **n**umber of cycles

4. Results and Discussion

4.1 Test Results

The results of this study are summarized in Table 10.

Table 10: Results of cyclic testing program

Test #	Test Name	Initial D_R	Final D_R	Target CSR	CSR at 5% DA	N overall	N 5% DA	r_u	ε_{vol} [%]
1	CYC-09-20	59	68	0.12	0.108	18	15	0.92	3.4
2	CYC-09-22	56	68	0.1	0.9	47	44	0.98	4.51
3	CYC-09-23	57	67	0.08	0.078	113	110	0.95	3.93
4	CYC-09-26	41	61	0.12	0.108	22	20	0.96	5.18
5	CYC-09-27	45	62	0.1	N.A.	12	N.A.	0.76	1.01
6	CYC-09-28	53	72	0.1	N.A.	21	N.A.	0.97	2.33
7	CYC-09-19	49	57	0.12	N.A.	4	N.A.	0.2	0.13
	CYC-09-19b		58	0.12	0.112	20	17	0.93	3.45
8	CYC-09-21	61	67	0.12	N.A.	4	N.A.	0.21	0.15
	CYC-09-21b		68	0.12	N.A.	10	N.A.	0.34	0.2
	CYC-09-21c		69	0.12	N.A.	15	N.A.	0.31	0.15
9	CYC-09-24	64	70	0.14	N.A.	4	N.A.	0.19	0.19
	CYC-09-24b		71	0.14	N.A.	10	N.A.	0.17	0.14
	CYC-09-24c		72	0.14	N.A.	30	N.A.	0.59	0.32

Legend:

D_R	: Relative density
Initial D_R	: After MMT method sample preparation
Final D_R	: Before cyclic loading
CSR @ 5%DA	: Average cyclic stress ratio applied to the sample up to the number of cycles that the test was stopped or when it reached liquefaction
DA	: Double amplitude strain
N	: Number of cycles of uniform loading
r_u	: Residual pore pressure ratio before at the end of undrained loading
ε_{vol}	: Volumetric strain
N.A.	: Not Applicable

Tests 1 through 6 were loaded in a single cyclic stage, either to liquefaction or a value of $r_u < 1$. Tests 7, 8, and 9 were loaded in two or more stages, with reconsolidation occurring after each stage. In these tests the number of load cycles was predetermined, with the number increased for each subsequent stage so that the pore pressure ratio in the retested samples would increase. It was assumed that no pre-straining or stiffening effect would affect the r_u results for these stages. Figure 19 illustrates the results from Test No. 4 (CYC-09-26). All the test results are included in Appendix A.

In Figure 19a, the cyclic deviator stress $(\sigma_d)[kPa]$, axial strain $(\varepsilon_a)[\%]$, double-amplitude strain $(\varepsilon_{\mathrm{DA}})[\%]$, pore pressure ratio (r_u) and displacement $[mm]$, are plotted versus

number of cycles. In Figure 19b, shear stress is compared to normal stress and the deviator stress to axial strain.

The pore pressure ratio, r_u, in Figure 19a shows a progressive increase with each cycle of loading. Soil liquefaction describes a phenomenon where a saturated cohesionless soil under undrained conditions loses its strength and stiffness in response to an applied stress (i.e. earthquake). It is reached when either r_u equals one, or the strain amplitude increases to an axial strain of about 5% (Ishihara, 1993). In test 4 the r_u almost reached 1 at 20 cycles, but at this moment, the sample failed.

The variation of deviator stress with number of cycles shows a continuous sinusoidal curve until failure occurred. At failure, the cyclic load could no longer be maintained by the hydraulic system and the applied stresses were reduced. Also at failure, axial strain and double amplitude increased significantly.

The axial strain deviator stress relationship shown in Figure 19b illustrates the deformation of the sample during each cycle of loading. Positive axial strain showscompression of the sample and negative axial strain corresponds to extension of the sample. This graph shows that the sample in test 4 was less stiff in extension than in compression.

Figure 20 shows the results of the undrained cyclic triaxial tests 1 through 4. These samples were loaded until liquefaction occurred. The final relative density (after consolidation) of these samples ranged from 61 to 68%. It can be observed from this figure that the lower the CSR the greater the number of cycles to failure. For example, sample 23, which was sheared at a CSR=0.08 liquefied at 110 cycles whereas sample 20, which was sheared at a CSR=0.12 liquefied at 15 cycles. No clear trend was observed in terms of relative density.

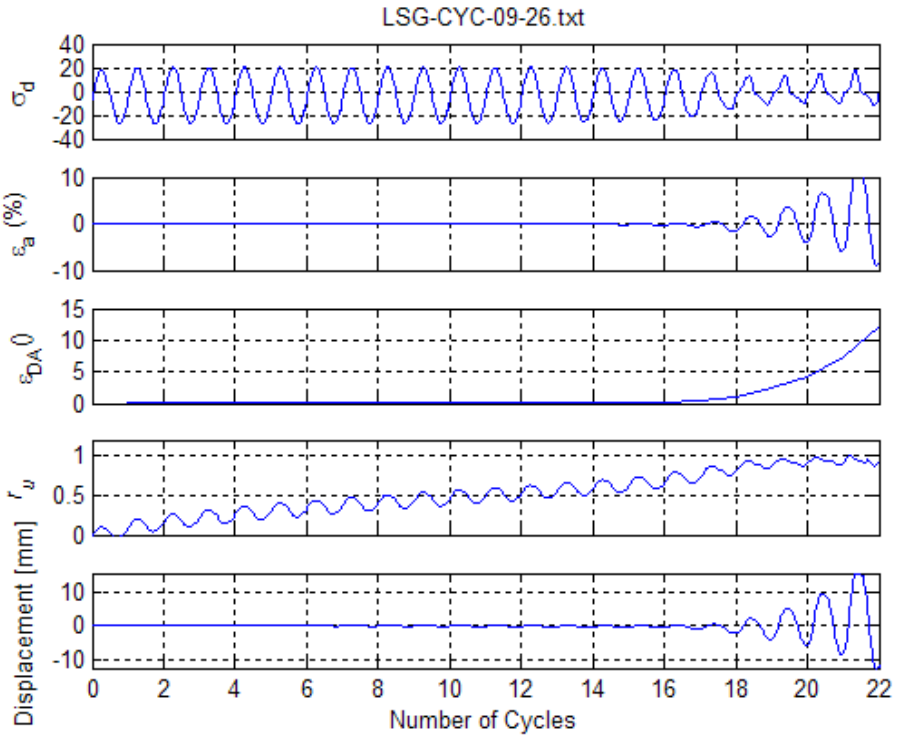

(a.)

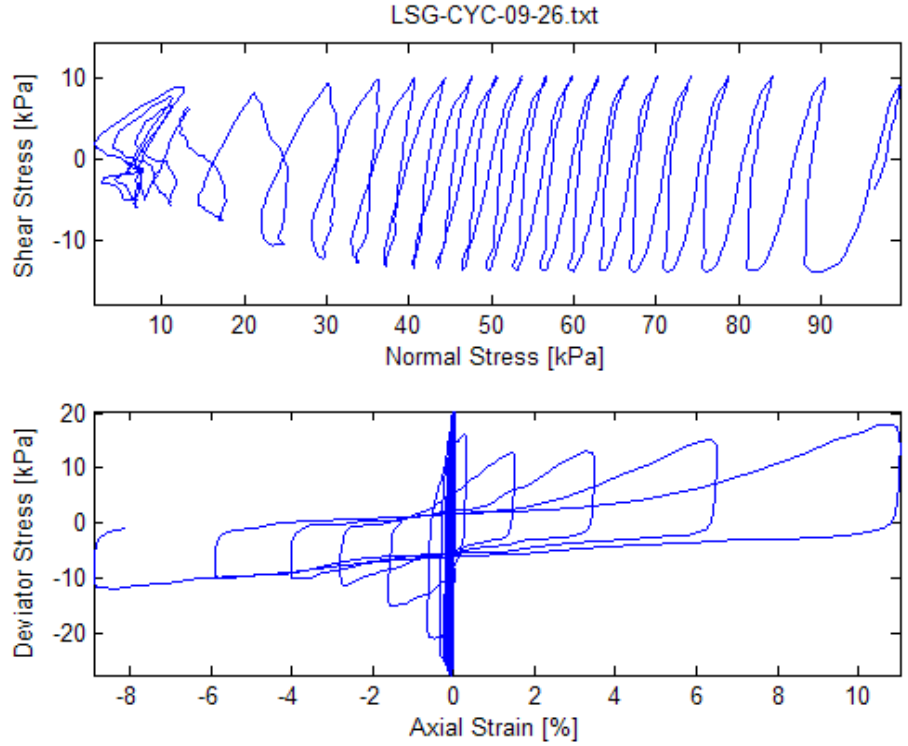

(b.)

Figure 19: Typical results of a cyclic triaxial test showing a.) the variation of properties with cycles of loading, and b.) stress-strain behavior.

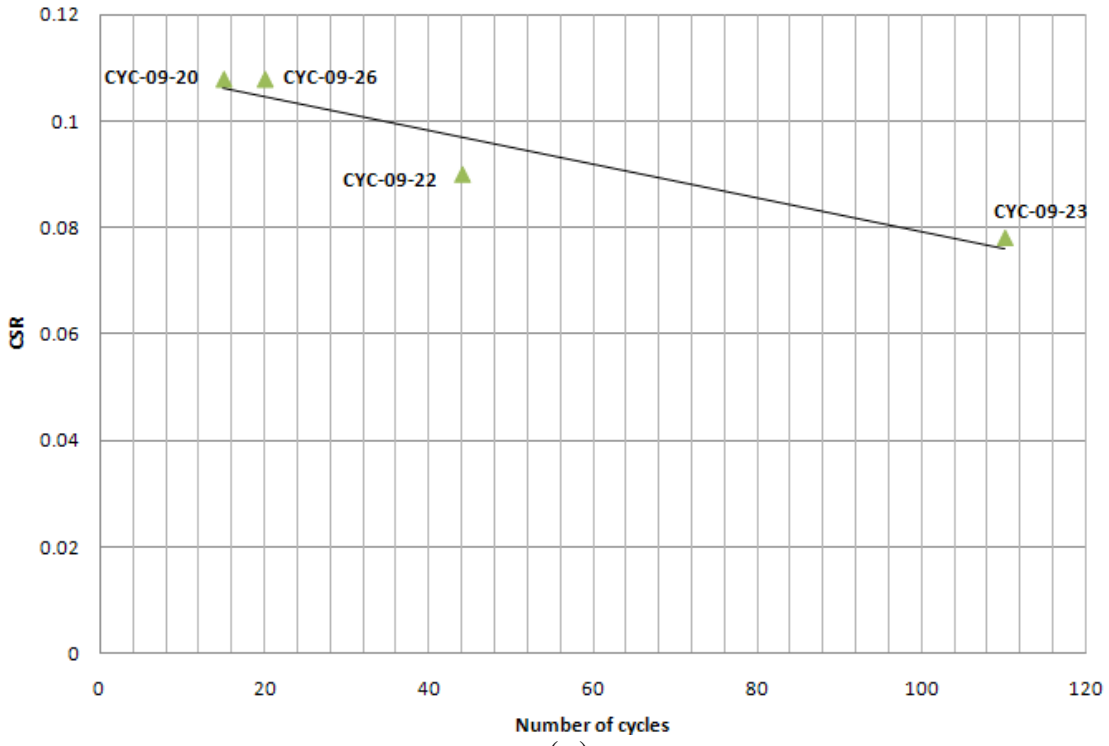

(a.)

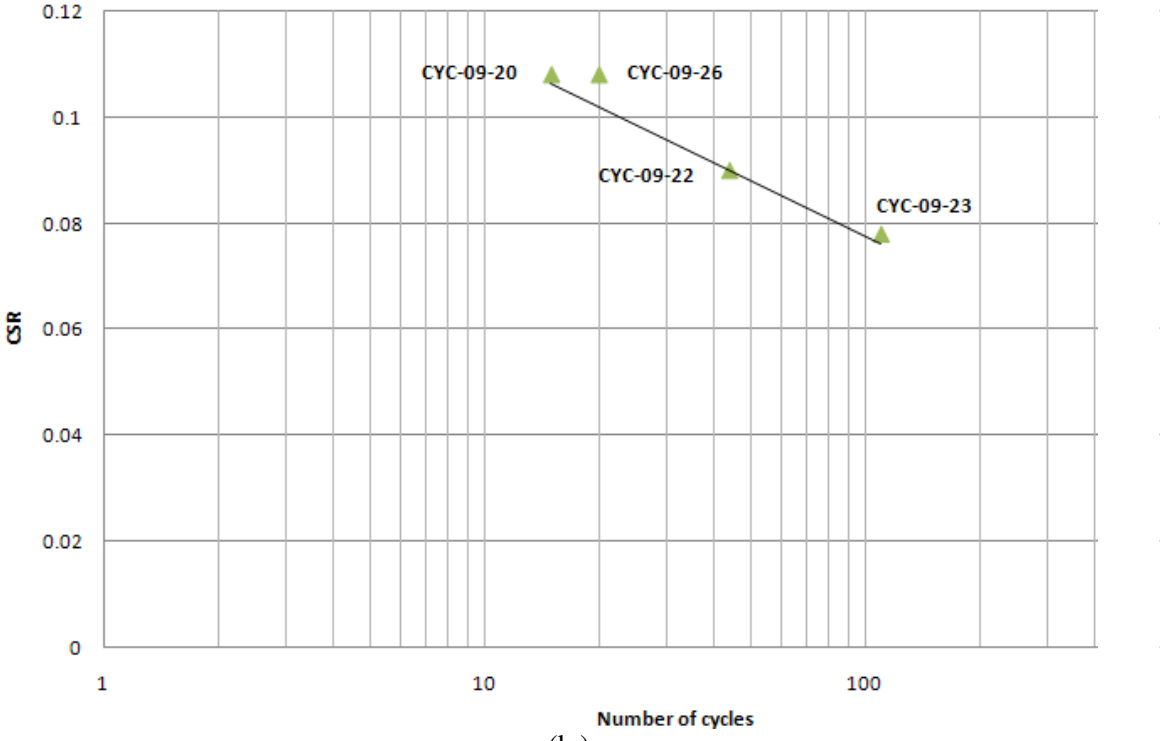

(b.)

Figure 20: Cyclic stress ratio versus number of cycles to 5% double amplitude strain for samples of silt in this study. The relative densities of these samples ranged from 61 to 68%.

4.2 Results of Volume Change due to Pore Pressure Dissipation

The results of the nine tests were compiled to determine a relationship between pore pressure ratio at the end of cyclic loading and volumetric strain for different values of relative density.

Tests 1 through 6 were loaded in a single cyclic stage, either to liquefaction or a value of $r_u < 1$. The loading caused pore pressure, which then caused volumetric strain during subsequent drainage. Figure 21 shows the relationship between the pore pressure ratio and volumetric strain, for specimens subjected to a confining stress of 100 kPa**.**.

In Figure 21, the upper and lower bounds were incorporated to show the range at which the volumetric strains were anticipated, given the limited number of tests.

Tests 7, 8, and 9 were loaded in two or more stages. The aim was to create more data with a smaller number of samples. The results of both tests were combined and are shown inFigure 22.

These results suggested the following:

- Figures 21 and 22 show a similar trend to the work of Lee and Albaisa (1974) (Figure 15). Lee and Albaisa analyzed earthquake induced settlements in saturated sands. They demonstrated that the cyclic strength of sand increased with increasing relative density. For relative densities in the range of 30 to 80%, regardless of the confining pressure, the volumetric strain of Monterey sand was a maximum of 1 %.
- Although the trend presented is similar to Lee and Albaisa, the magnitude of volumetric strain was significantly higher for the silt (up to 5%) than for sands (typically less than 1%). It is not clear whether this is a consistent trend for silts or whether the different boundary conditions (isotropic in this study vs. one-dimensional compression) are responsible for the results.

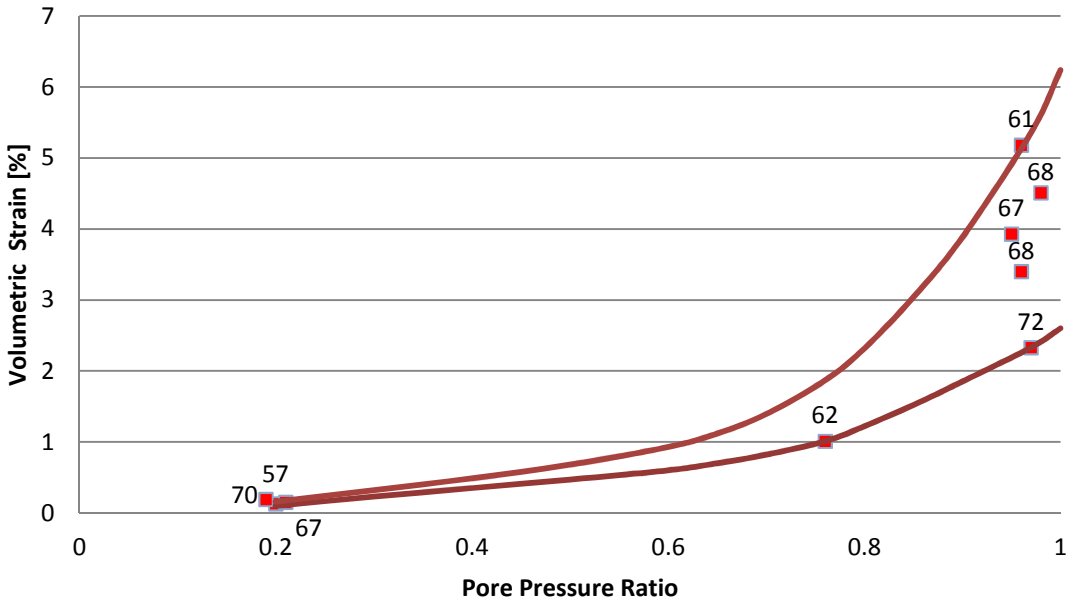

Figure 21: Relationship between volumetric strain and pore pressure ratio for samples with relative densities (shown next to the data points) ranging from 57 to 72%. Only results from single cyclic loading stages are included.

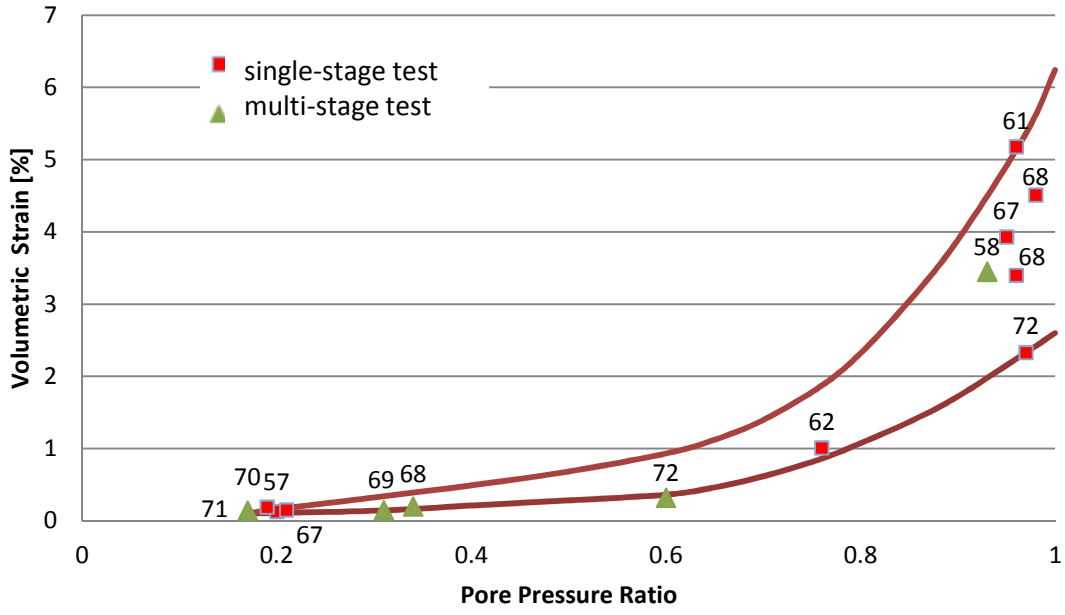

Figure 22: Relationship between volumetric strain and pore pressure ratio for samples with relative densities (shown next to the data points) ranging from 57 to 72%. Results from both single cyclic loading stage and multiple stage tests are included.

4.3 Issues that Affect the Quality of the Results

There were a number of issues during laboratory testing for this study on silt that influenced the quality of the results. These issues are presented here because they contributed to the outcome and, therefore, should be kept in mind when analyzing the data. In addition, these issues may be of importance for further research in this area. A brief overview of issues that affected the quality of the results will follow.

There was not a clear trend in the effect of relative density on r_u and volumetric strain. This is most likely due to a problem with the sample preparation methodology. Samples were prepared to the same water content (18%) regardless of the initial density. Samples should have been prepared to a constant degree of saturation (55% according to Bradshaw and Baxter, 2007) instead. At 18% water content, the initial degrees of saturation varied with density and the initial fabric was likely different for the different densities. This would explain why some of the samples exhibited different amounts of volume change during inundation.

Pore pressures after cyclic loading were not always equivalent to those prior to drainage. In tests 5 and 6, cyclic loading was stopped at a pore pressure ratio smaller than 1. After cyclic loading was stopped, pore pressure at the ends continued to increase. This increase in pore pressure, after cyclic loading, could only have come from pore pressure within the sample. This was consistent with suggestions made by Bradshaw (2006) who believed that such behavior of silt was attributed to a non-uniform distribution of pore pressure due to low permeability within the sample. Zhou et al. (1995) also showed that in isotropically consolidated tests of silt, pore pressures measured at the bottom and top of the sample were lower than those measured in the interior of the sample. Thus, the volumetric strain of the sample is dependent on pressures within the sample before drainage, and not after cyclic loading. To make the comparative data for Figure 21, pore pressure before drainage was chosen rather than pore pressure after cyclic loading.

In 1976, Silver et al. provided a standard for cyclic triaxial testing. This standard recommends a loading frequency of 1 Hz. In this laboratory study a loading frequency of 0.5Hz was chosen. A smaller loading frequency was chosen so that pressure build-up would be slower. This was favorable, as it was of interest to stop the cyclic loading at various pore pressure levels. Changes of loading frequency were not believed to have any influence on the test results, because Riemer et al. (1994) proved that effect of frequency on the number of cycles to liquefaction at a given CSR was not significant in stress controlled loading. The study of Riemer et al. was undertaken using Monterey 0 clean sand.

For this study, silt samples were tested at 2, 1 and 0.5 Hz to ensure that there are no loading frequency effects in cyclic triaxial tests on silt. The obtained test results were inconclusive in this regard. Before further tests are conducted it has to be evaluated if there is a loading frequency effect on the results of cyclic triaxial testing for silt.

In 2006, Bradshaw had obtained silts from Wellington Avenue and Olneyville construction sites. In addition, Bradshaw had developed the MMT method as an alternative for liquefaction testing of silts. For his testing, cyclic triaxial tests with the two silts were performed. The material used in this study was blended silt consisting of the two original silts. For this

laboratory study, all samples were reconstituted in accordance with the MMT method. There was not an agreement between the results of this study and the results obtained by Bradshaw (2006). This could be due to using a blended material, but is more likely that using constant water content instead of constant saturation resulted in different fabric and different strengths.

5. Recommendations

The influence of relative density on volumetric strain for samples at the same pore pressure ratio was studied. Unfortunately, no conclusion confirming the influence of relative density could be drawn because the number of tests did not generate enough results, even when samples were reused to create more data points. For samples with relative densities of 57 to 72 %, the increase in volumetric strain was small up to a pore pressure ratio of 0.6. Volumetric strain below this pore pressure appeared to be independent of relative density. Further research is needed to obtain results, which include the effects of density.

Non-uniform pore pressures within the silt samples also likely affected the results. Whenever tests were manually terminated at pore pressure ratios close to 1,it was observed that the pore pressures continued to increase after cyclic loading. Further tests with an internal pore pressure needle should be performed to prove that increases in pore pressures after cyclic loading is the result of equalization of greater pore pressures from the center of the sample to the ends.

The presence of non-uniform pore pressures suggests that there could be an effect of loading frequency on the cyclic behavior of the Providence silts. This possibility should be investigated further as it could significantly affect the evaluation of cyclic resistance for silty soils.

6. Conclusions

When a pile or sheet pile is installed, vibrations are generated in the nearby ground. This vibration can cause damage to neighboring structures and settlement of adjacent ground. Before any pile construction is undertaken engineers have to estimate what the risks and dangers of such installation are. In this phase of planning they have to make decisions, which will have consequences for the rest of the project. Currently, there is no general prediction method for estimating the settlement of adjacent ground in silt.

The objectives of this study were to perform a detailed review of the literature regarding pile driving-induced settlements and to develop a laboratory testing program to quantify the relationship between cyclic loading, generation of pore pressures, and the resulting volume changes in silts.

For the literature review, seven case studies of settlement due to pile driving were presented and summarized. Only the case study from Bradshaw et al. (2007) dealt with settlement from pile driving in silt. A summary of six methods of settlement prediction and a critical comparison of those methods were also presented. It was noted that all methods were derived from sand, and that there was no appropriate method for general prediction of settlement or method for prediction of silt settlement.

In the second part of this study nine cyclic triaxial tests were performed to predict the volume change of the silt due to dissipation of excess pore pressures generated during cyclic loading. An important milestone in this study was thedevelopment of a methodology for measuring volume changes throughout the entire test and in particular relating volume change during reconsolidation to pore pressures generated during undrained cyclic loading.The results are qualitatively similar to published work by Lee and Albasia for sands.

Preparing samples to constant water content rather than a constant degree of saturation likely affected the sensitivity of the results to relative density. This is because samples prepared to water content of 18% exhibited significant volume change during inundation.

The modeling of the potential settlement of adjacent ground was completed as part of a saparate RIDOT grant.

The overall approach developed in this study to estimate the volume change behavior of silts following cyclic loading was ultimately successful, and the results of volumetric behavior obtained in this study provide a sound basis for further research into the settlement of adjacent ground due to pile driving in silt.

7, List of References

ASTM D854 – 06 Standard Test Methods for Specific Gravity of Soil Solids by Water Pycnometer.

ASTM D1557 – 07 Standard Test Methods for Laboratory Compaction Characteristics of Soil Using Modified Effort.

ASTM D 4254 Standard Test Methods for Minimum Index Density and Unit Weight of Soils and Calculation of Relative Density.

Attewell, P.B., Selby, A.R., and O'Donell, L. (1992). "Tables and Graphs for the Estimation of Ground Vibration from Driven Piling Operations." Geotechnical and Geological Engineering, 10 (1), 1992, pp. 61-87.

Bement, R. A. P., and Selby, A. R. (1997). "Compaction of Granular Soils by Uniform Vibration Equivalent to Vibrodriving of Piles." Geotechnical and Geological Engineering, 15, 1997, pp. 121-143.

Bradshaw, A. S. (2006). "Liquefaction Potential of Non-Plastic Silt." Ph.D. dissertation, University of Rhode Island.

Bradshaw, A.S., and Baxter, C.D.P (2007). "Sample Preparation of Silts for Liquefaction Testing." ASTM Geotechnical Testing Journal, 30(4), pp. 324-332.

Bradshaw, A.S., Miller, H.J., and Baxter, C.D.P. (2007). "A Case Study of Construction- Related Ground Movements in Providence Silt." Proceeding of the Sessions of the FMGM 2007 Conference, American Society of Civil Engineers, Boston, Massachusetts, pp. 1-8.

Castro, G. (1975). "Liquefaction and Cyclic Mobility of Saturated Sands." Journal of the Geotechnical Engineering Division, 101(6), pp. 551-569.

Clough, G. W., and Chameau, J.L. (1980). "Measured Effects of Vibratory Sheetpile Driving." Journal of the Geotechnical Engineering Division, Vol. 106, No. 10, October 1980, pp. 1081-1099.

Dalmatov, B. I., Ershov, V. A. and Kovalevsky, E. D. (1968). "Some Cases of Foundation Settlement in Driving Sheeting and Piles." Proc. Of Symposium on Wave Propagation and Dynamic Properties of Earth Materials, University of New Mexico, Albuquerque, NM, pp. 607 – 613.

Drabkin, S., Lacy, H., and Kim, D.S., (1996). "Estimating Settlement of Sand Caused by Construction Vibration." Journal of Geotechnical Engineering, November 1996, pp. 920-928.

Ershov, V.A., (1965). "Shearing Strength of San Soil Drawn into Vibration. Construction Engineering Materials and the Carrying out of Work." Reports to 1st Scientific Conference of Young Scientists- Builders in LISI, Leningrad.

Ishihara, K (1993). "Liquefaction and flow failure during earthquakes," Géotechnique 43, No. 3, pp. 351-415.

Ishihara, K., and Yoshimine, M. (1992). "Evaluation of Settlements in Sand Deposits Following Liquefaction During Earthquakes." Soils and Foundations, 32(1), pp. 173-188.

Ladd, R. S., (1978). "Preparing Test Specimens Using Undercompaction." Geotech, Test. J. ASTM, Vol. 1, No. 1, pp. 16-23.

Lacy, S. H., and Gould, J. P. (1985). "Settlement from Pile Driving in Sands." Vibration Problems in Geotechnical Engineering. Proceedings of a Symposium by the Geotechnical Engineering Div. in conjunction with the ASCE Convention in Detroit, Mich., Oct. 22, 1985, pp. 152-173.

Leathers, F.D. (1994). "Deformations in Sand Layer during Pile Driving." Proceedings of Settlement ´94, Geotechnical Special Publication 40, ASCE, June 1994, pp. 257-268.

Lee, K. and Albasia, A. (1974). "Earthquake Induced Settlements in Saturated Sands." Journal of the Geotechnical Engineering Division, ASCE, Vol. 100, GT 4, pp. 387-405.

Linehan, P. W., Longinow, A., and Dowding, C. H. (1992). "Pipe Response to Pile Driving and Adjacent Excavation." Journal of Geotechnical Engineering, Vol. 118, No. 2, February, 1992, pp. 300-316.

Lukas, R.G. and Gill, S.A., (1992). "Ground Movement from Piling Vibrations." Proceedings Conference Piling: European practice and worldwide trends, London 1992, pp. 163 -169.

Malvern (2005). "Mastersize 2000 – Integrated systems for particle sizing." Malvern Instruments Limited, Copyright 2005.

Maslov, N.N., (1959). "Stability Conditions of Sautrated Sands", Gosenergoizdat, Moscow.

Massarsch, K.P. (1992). "Static and Dynamic Soil Displacements Caused by Pile Driving." Proceedings 4th Int. Conference Application of Stress-wave Theory to Piles, The Hague 1992, pp. 15-24.

Massarsch, K.P. (2000). "Settlements and Damage Caused by Construction-induced Vibrations." Proceeding, Intern. Workshop Wave 2000, Bochum, December 2000, pp. 299-315.

Massarsch, K.P. (2004). "Vibrations Caused by Pile Driving." The Magazine of the Deep Foundations Institute, Fall 2004, pp. 39-42.

Meijers, P. (2007). “Settlement During Vibratory Sheet Piling.” Ph.D. Dissertation (van Tol, A.F., Advisor),TechnischeUniversiteit Delft, pp. 19-32.

Mohamed, R., and Dobry, R. (1987). “Settlement of Cohesionless Soils Due to Pile Driving.” Proceedings, 9th Southeast Asian Geotechnical Conference, Bangkok, Thailand, pp. 7-23.

Picornell, M., and Del Monte, E. (1985). “Pile Driving Induced Settlements of a Pier Foundation.” Vibration problems in geotechnical engineering, ASCE, October 1985, pp 174-186.

Polito, C.P. (1999). “The Effects of Non-Plastic and Plastic Fines on the Liquefaction of Sandy Soils.” PhD. Dissertation, Virginia Polytechnic Institute, Vicksburg, VA.

Riemer, M.F., Gookin, W.B., Bray, J.D. and Arango, I. (1994).“Effects of Loading Frequency and Control on the Liquefaction Behavior of Clean Sands."Geotechnical Engineering Report No. UCB/GT/94_07, University of California, Berkeley, December, 1994.

Seed, H.B., and Lee, K.L. (1966). “Liquefaction of saturated sands during cyclic loading.” Journal of the Soil Mechanics and Foundations Division, 92(6), pp. 105-134.

Seed, H. B., and Silver, M. L. (1969). “The Behavior of Sands Under Seismic Loading Conditions.” Report No EERC 69-16. Dez. 1969, California University Berkles Earthquake Engineering Research Center.

Seed, H. B., and Silver, M. L. (1972). “Settlements of Dry Sand During Earthquakes.” Journal of the Soil Mechanics and Foundation Division, Proceedings ASCE, Vol. 98, pp. 381- 396.

Silver, M. L., Chan, C. K., Ladd, R. S., Lee, K. L., Tiedemann, D. A., Townsend, F. C., Valera, J. E., and Wilson, J. H. (1976). “Cyclic triaxial strength of standard test sand.” Journal of the Geotechnical Engineering Division, 102(GT5), pp. 511-523.

Silver, M. L. and Seed, H. B. (1971), “Volume Changes in Sands during Cyclic Loading.” Journal of the Soil Mechanics and Foundations Division, Vol. 97, No. 9, September 1971, pp. 1171-1182.

Youd, T. L. (1972). “Compaction of Sands by Repeated Shear Straining.” Journal of the Soil Mechanics and Foundation Division, Proceedings ASCE, Vol. 98, pp. 709-725.

Zhou, J., Lee, W., and Zhou, K. (1995). “Dynamic Properties and Liquefaction Potential of Silts.” Proceedings of the 1995 International Conference on Earthquake Geotechnical Engineering, Vol. 2, pp. 833-838.

Appendices - Results of Cyclic Triaxial Testing Program

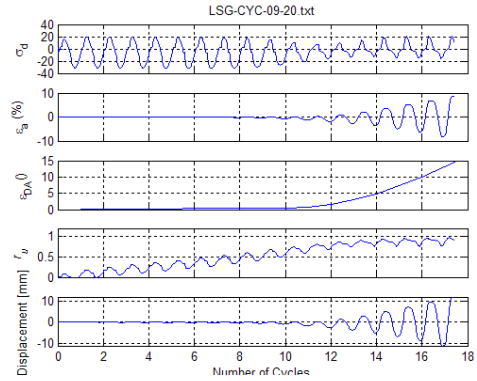

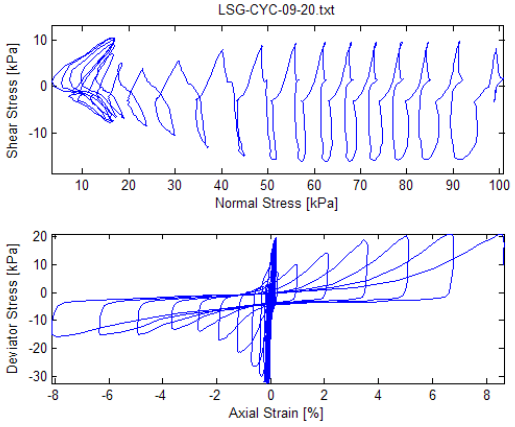

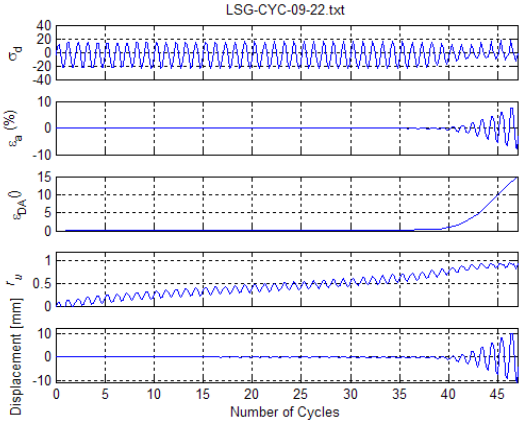

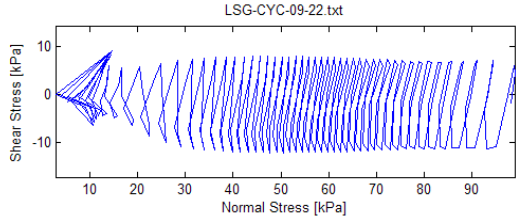

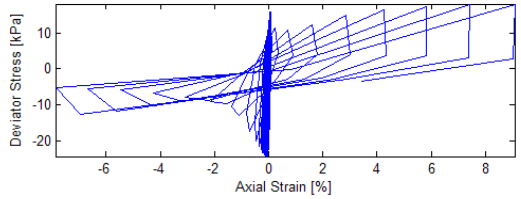

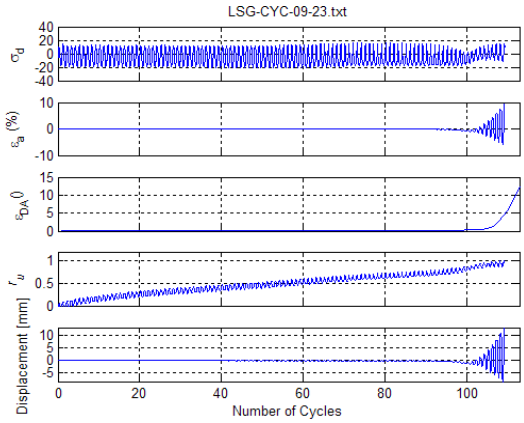

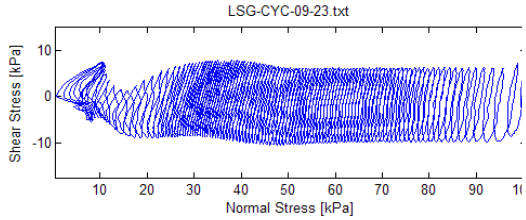

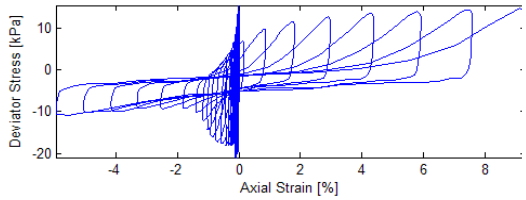

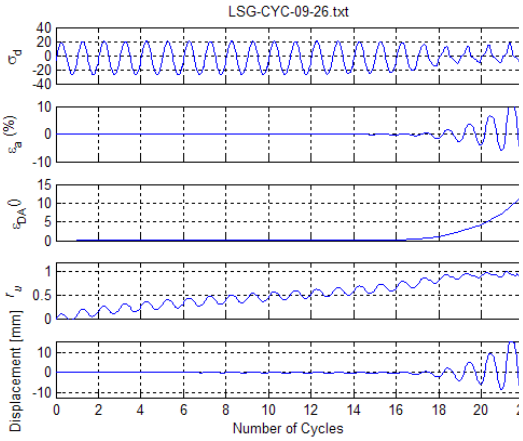
LSG-CYC-09-26.txt
σd
εa (%)
εDA ()
ru
Displacement [mm]
Number of Cycles

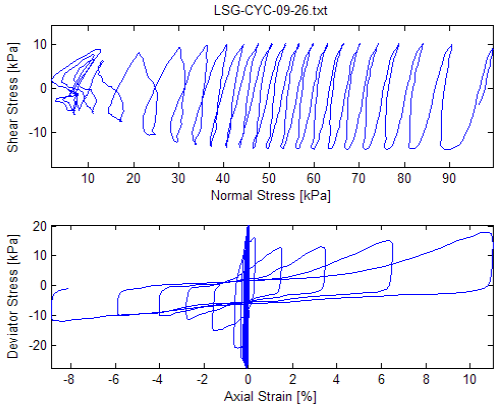
LSG-CYC-09-26.txt
Shear Stress [kPa]
Normal Stress [kPa]
Deviator Stress [kPa]
Axial Strain [%]

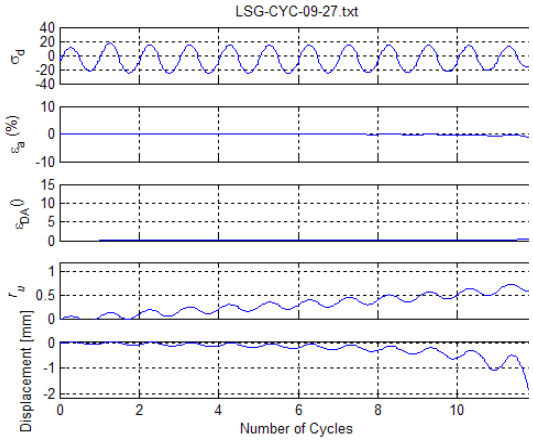
LSG-CYC-09-27.txt
σd
εa (%)
εDA ()
ru
Displacement [mm]
Number of Cycles

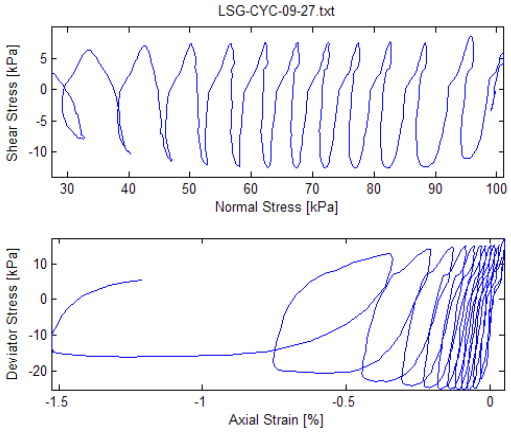
LSG-CYC-09-27.txt
Shear Stress [kPa]
Normal Stress [kPa]
Deviator Stress [kPa]
Axial Strain [%]

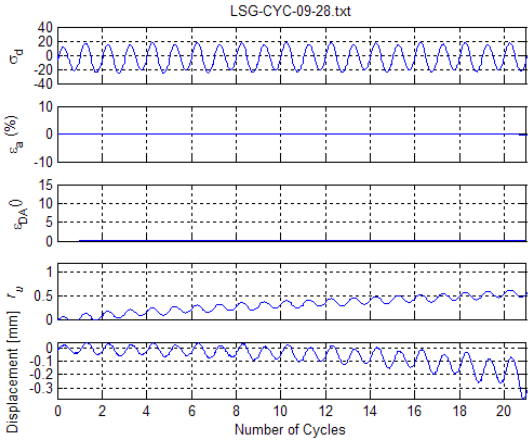
LSG-CYC-09-28.txt
σd
εa (%)
εDA ()
ru
Displacement [mm]
Number of Cycles

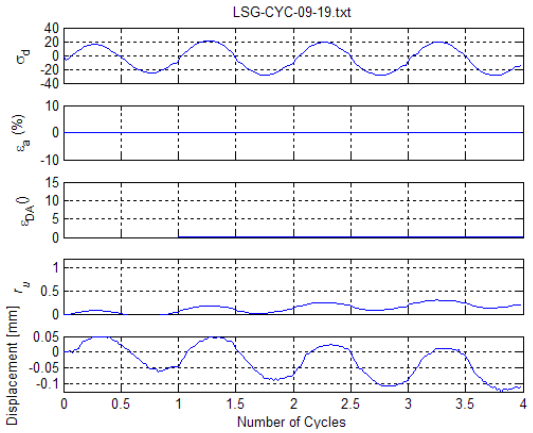
LSG-CYC-09-19.txt
σd
εa (%)
εDA()
ru
Displacement [mm]
Number of Cycles

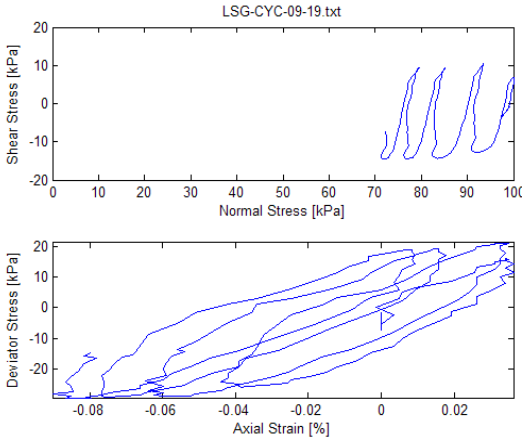
LSG-CYC-09-19.txt
Shear Stress [kPa]
Normal Stress [kPa]
Deviator Stress [kPa]
Axial Strain [%]

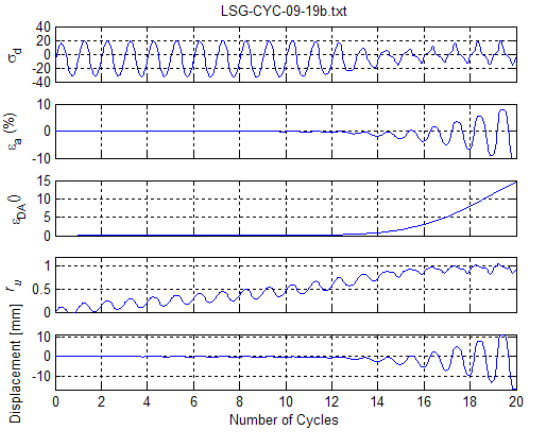
LSG-CYC-09-19b.txt
σd
εa (%)
εDA()
ru
Displacement [mm]
Number of Cycles

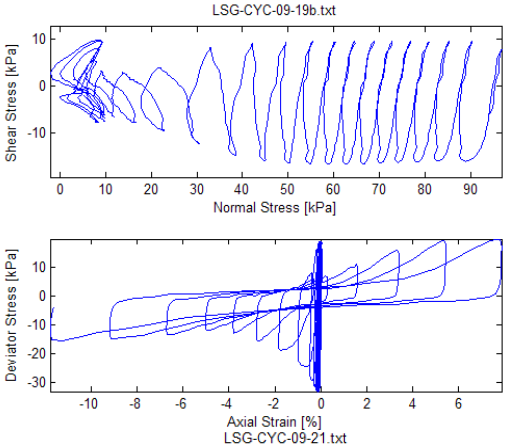
LSG-CYC-09-19b.txt
Shear Stress [kPa]
Normal Stress [kPa]
Deviator Stress [kPa]
Axial Strain [%]

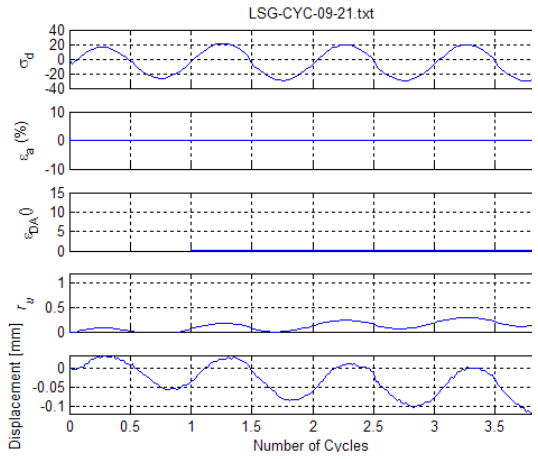
LSG-CYC-09-21.txt
σd
εa (%)
εDA()
ru
Displacement [mm]
Number of Cycles

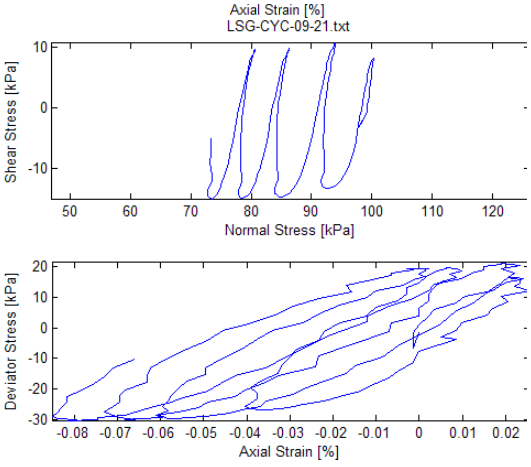
LSG-CYC-09-21.txt
Shear Stress [kPa]
Normal Stress [kPa]
Deviator Stress [kPa]
Axial Strain [%]

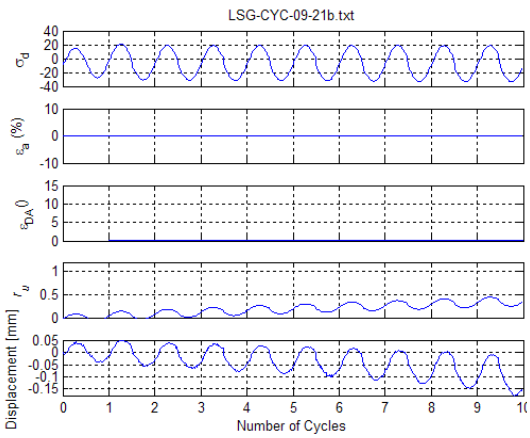
LSG-CYC-09-21b.txt
σd
εa (%)
εDA ()
ru
Displacement [mm]
Number of Cycles

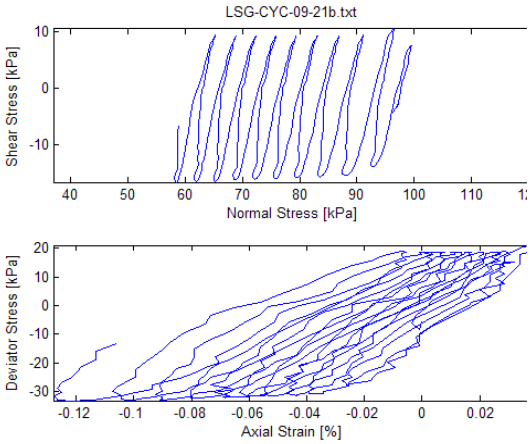
LSG-CYC-09-21b.txt
Shear Stress [kPa]
Normal Stress [kPa]
Deviator Stress [kPa]
Axial Strain [%]

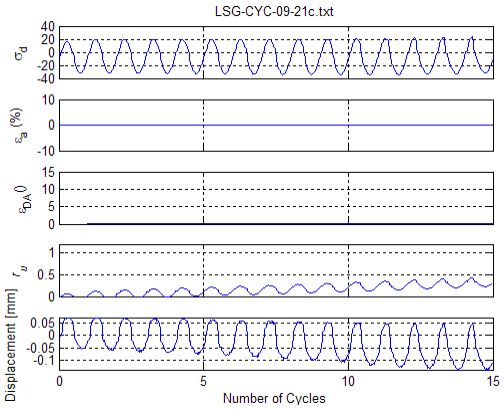
LSG-CYC-09-21c.txt
σd
εa (%)
εDA ()
ru
Displacement [mm]
Number of Cycles

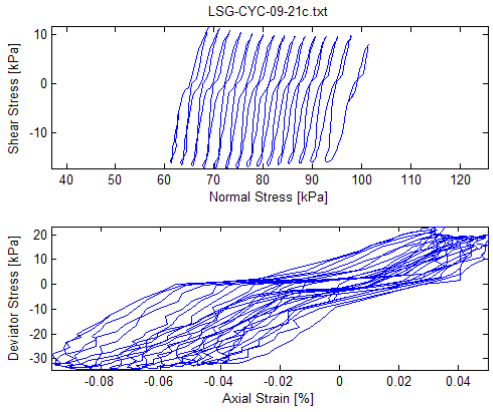
LSG-CYC-09-21c.txt
Shear Stress [kPa]
Normal Stress [kPa]
Deviator Stress [kPa]
Axial Strain [%]

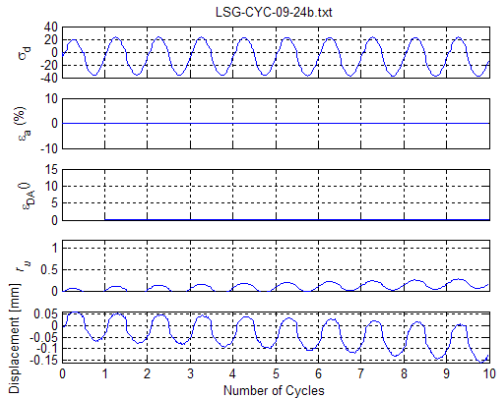
LSG-CYC-09-24b.txt
σd
εa (%)
εDA ()
ru
Displacement [mm]
Number of Cycles

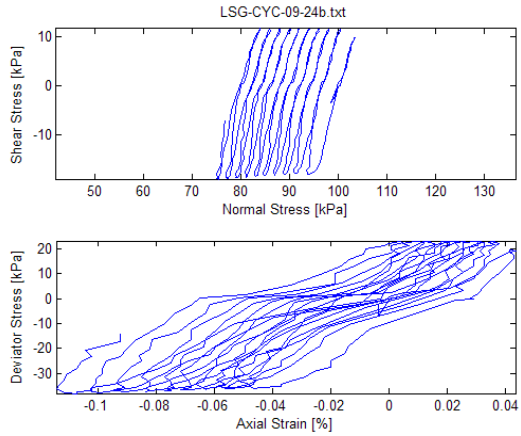
LSG-CYC-09-24b.txt
Shear Stress [kPa]
Normal Stress [kPa]
Deviator Stress [kPa]
Axial Strain [%]